FACULTY OF INFORMATION TECHNOLOGY AND ELECTRICAL ENGINEERING

Eemeli Ristimella

SMART LUMINAIRE POSITIONING AND LIGHTING CONTROL IN COLLABORATIVE SPACES

Master's Thesis
Degree Programme in Computer Science and Engineering
September 2020

Ristimella E. (2020) Smart Luminaire Positioning and Lighting Control in Collaborative Spaces. University of Oulu, Degree Programme in Computer Science and Engineering, 63 p.

ABSTRACT

Smart lighting systems have become more common as they provide energy savings with various occupancy detection methods and better lighting control opportunities for users. This thesis explores two aspects of these smart lighting systems, configuration and control, by utilizing an ActiveAhead controlled smart luminaire installation at the University of Oulu.

Smart luminaire identification is a common configuration task that needs to performed before being able to control the individual luminaires and can be especially tedious with large installations. However, this task can be partly automated by positioning the smart luminaires based on passive infrared (PIR) sensors or the received signal strength indicators (RSSI) the luminaires broadcast with Bluetooth Low Energy (BLE) advertisements. For PIR sensor-based positioning, a centroid-based method is presented and evaluated with two datasets reflecting a typical and optimal scenarios of triggering the sensors. For RSSI-based positioning, a log-distance path loss distance estimation with mean squared error (MSE) based position optimization is presented and evaluated. Moreover, relevant literature concerning the RSSI-based device positioning is discussed.

Second, the design, implementation and evaluation of a lighting control prototype for collaborative spaces are presented. The prototype uses near-field communication (NFC) tags to indicate the user position and to initiate a lighting preference input to an Android application. The user preferences are transmitted to a local server responsible for the control logic and communication with the luminaires. The potential conflicts between users are resolved with distance weighted preference averaging, which makes the prototype especially convenient for cases where the users share the surrounding luminaires with others. Furthermore, related smart lighting control systems are compared.

Keywords: PIR sensors, RSSI, locationing, smart lighting control

Ristimella E. (2020) Älyvalaisinten paikantaminen ja valaistuksen säätö yhteistyötiloissa. Oulun yliopisto, Tietotekniikan tutkinto-ohjelma, 63 s.

TIIVISTELMÄ

Älykkäät valaistusjärjestelmät ovat yleistyneet mahdollistaen energiansäästöt useilla läsnäolon tunnistusratkaisuilla ja paremmat valaistuksen säätömahdollisuudet käyttäjille. Tämä työ käsittelee älyvalaistusjärjestelmiä kahdesta näkökulmasta hyödyntäen ActiveAhead älyvalaisinasennusta Oulun yliopistossa.

Älyvalaisinten paikan tunnistaminen on yleinen konfigurointivaihe ennen kuin yksittäisiä valaisimia on mahdollista säätää ja se voi osoittautua erityisen työlääksi suurissa asennuksissa. Tämä vaihe on kuitenkin mahdollista automatisoida paikantamalla älyvalot hyödyntäen PIR-liiketunnistimia tai vastaanotetun signaalin voimakkuutta (RSSI), joita valaisimet lähettävät matalanenergian (BLE) Bluetoothin mainosviesteillä. PIR-liiketunnistimiin pohjautuvaan paikantamiseen esitellään painopisteeseen perustuva metodi, joka myös evaluoidaan kahdella datasetillä, jotka kuvaavat yleistä ja optimaalista PIR-liiketunnistimien laukaisua. RSSI pohjaiseen paikantamiseen esitellään ja arvioidaan metodi, joka hyödyntää logaritmisen signaalin vaimenemisen etäisyys-mallia ja keskimääräiseen neliövirheeseen perustuvaa paikan optimointia. Lisäksi esitellään käytettyjä menetelmiä RSSI-pohjaiseen paikantamiseen.

Toiseksi esitellään yhteisöllisiin työtiloihin tarkoitetun valaistuksensäätöprotyypin suunnittelu, toteutus ja evaluointi. Prototyyppi hyödyntää NFC (near field communication) tarroja käyttäjän sijainnin ilmaisuun ja valaistuspreferenssien syöttämisen osoittamiseen Android sovellukselle. Käyttäjäpreferenssit välitetään paikalliselle palvelimelle, joka vastaa ohjauslogiikasta ja viestinnästä valaisimien kanssa. Mahdolliset konfliktit käyttäjien välillä ratkaistaan etäisyydellä painotetulla keskiarvolla, mikä tekee prototyypistä kätevän erityisesti tilanteisiin missä käyttäjät jakavat ympäröivät valaisimet toistensa kanssa. Lisäksi vertaillaan muita älykkäitä järjestelmiä valaistuksen säätämiseen.

Avainsanat: PIR anturit, RSSI, älykäs valaistuksenohjaus

TABLE OF CONTENTS

FOREWORD

This Master's thesis was made for the Smart Campus project at the University of Oulu and has provided me with an opportunity to explore various technologies and topics.

I would like to express my gratitude to the Smart Campus project manager Risto Jurva for this opportunity to enhance my professional skills. Furthermore, I would like to thank my supervisors Susanna Pirttikangas, Ekaterina Gilman and Ari Pouttu for providing guidance during the process.

Finally, I would like to thank Helvar Oy Ab, especially Abdulla Ibrahim, Max Björkgren and Matti Vesterinen, for participating in forming the topic and helping with the control of the ActiveAhead equipped luminaires which were utilized in the thesis.

Helsinki, September 10th, 2020

Eemeli Ristimella

LIST OF ABBREVIATIONS AND SYMBOLS

AP	access point
APK	Android application package
API	application programming interface
BLE	Bluetooth low energy
CRUD	create, read, update and delete
GUI	graphical user interface
IOT	Internet of Things
IR	infrared
LCU	lighting controller unit
LOS	line-of-sight
HTTP	hypertext transfer protocol
MSE	mean squared error
NFC	near-field communication
PIR	passive infrared sensor
REST	representational state transfer
RF	radio frequency
RMSE	root mean squared error
RSS	received signal strength
RSSI	received signal strength indicator
SDK	software development kit
SLAM	simultaneous localisation and mapping
TTL	time-to-live
μ	mean
σ	standard deviation
d	Euclidean distance

1. INTRODUCTION

Artificial lighting is used in every modern building. Traditionally, luminaires are physically wired to form groups and controlled by a switch usually installed on a nearby wall. Recently, more intelligent lighting systems have emerged; they contain not only electrical lamps but also embedded chips and radio modules that enable the communication between the luminaires, and depending on the used communication technology, receiving lighting control commands from other smart devices. In addition to the smart control, some of these smart lighting systems utilize motion detectors and ambient light sensors to reduce energy consumption.

In this thesis, two aspects of these smart lighting systems are explored: First, the work aims to partly automate the positioning and identification process of the smart luminaires by utilizing the distance information from the transmitted received signal strength indicators (RSSI) and passive infrared (PIR) sensors, which are often installed in the luminaires. Secondly, an approach for the enabling users lighting control in collaborative environments is explored. ActiveAhead smart lighting system installation at the University of Oulu is utilized for these two purposes.

1.1. Smart Luminaire Positioning

In smart lighting systems, motion detectors are often used in lighting control to turn the lights off when people leave the space. However, a direct control over a specific luminaire is sometimes needed, for example, for adjusting the lighting directly at your desk. In order to control that specific luminaire, the knowledge of the identifier representing the luminaire in the group of other luminaires is required. The simplest way to match the luminaires with their identifiers is to manually send a flash command to every identifier, visually inspect the corresponding luminaires flashing in the space and mark down their locations. Needless to say, this manual identification can be tedious with larger installations. The manual luminaire identification is presented in Figure 1a.

The challenges in the manual luminaire identification were presented by the representatives of Helvar Oy Ab, who also suggested partly automating the luminaire identification by estimating the luminaire positions by using the Received signal strength (RSS) at the user smartphone and the triggers of the installed PIR sensors. They also suggested gathering a reference position for the user scanning the RSSI and triggering the PIR sensors with a help of a floorplan to make the luminaire positioning simpler. Furthermore, the positions of the unidentified luminaires, i.e., luminaire placeholders, were assumed to be known beforehand since they are often found in the floorplans. This semi-automated luminaire identification developed in this thesis, is illustrated in 1b.

1.2. Lighting Control Prototype for Collaborative Spaces

Controlling lighting is easy at home or other private space; you can simply toggle the lights on and off from the nearest switch. In a public space, the setting changes:

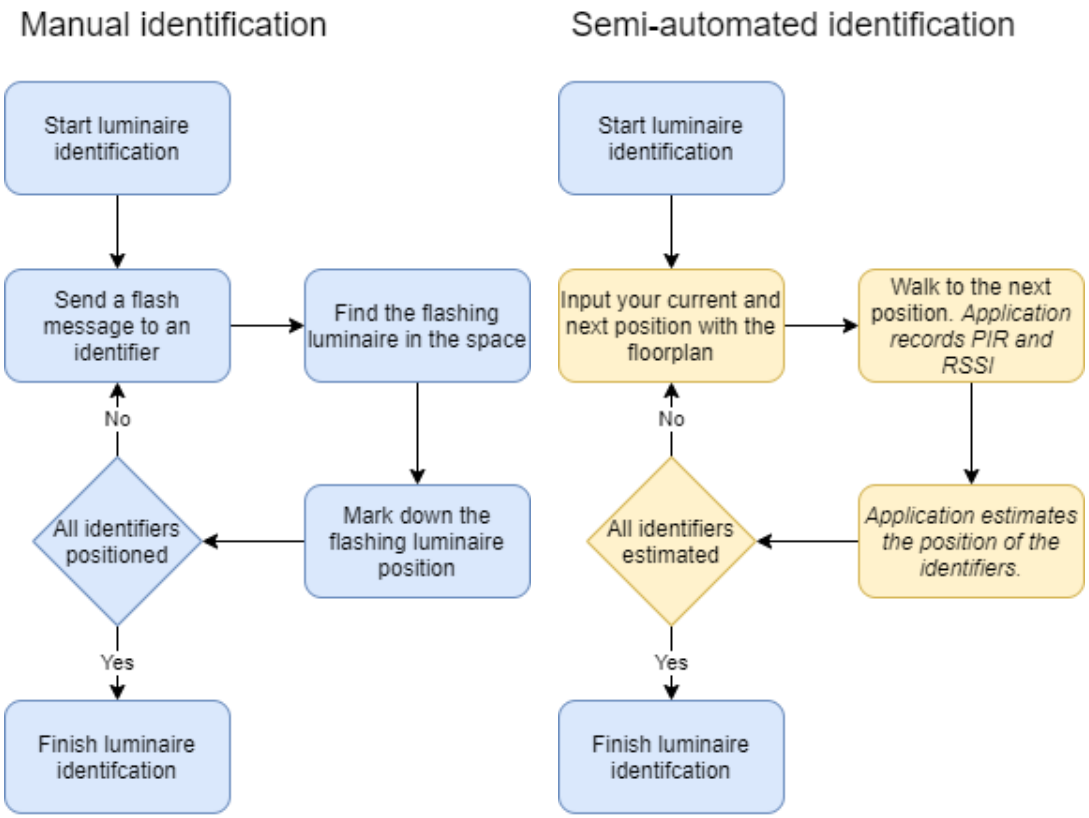

(a) Manual luminaire identification (b) Semi-automated luminaire identification concept.

Figure 1. The steps needed for manual and semi-automated luminaire identification concept.

switches can be hidden, and even if they are meant to be used, you may not want to make lighting adjustments since the other people present could have different lighting preferences than you. Despite these difficulties in adjusting lighting in public and collaborative spaces, users can benefit from having a personal lighting control [1] [2] [3].

Motivated by the previously done research and personal experiences when studying in a public space with only the default lighting available, the second goal of this thesis was to develop a prototype to enable personal lighting control in a public setting and evaluate user attitudes for such a system. The prototype was developed to a collaborative space, Business Kitchen, in Tellus[1] at the University of Oulu as part of a larger Smart Campus project.

[1] https://www.oulu.fi/tellusarena-fi/

2. RELATED WORK

This chapter takes a look at the relevant research related to the problem of smart luminaire positioning and previously implemented lighting control methods for collaborative spaces with Sections 2.1 and 2.2 respectively.

2.1. Smart Luminaire Positioning

A common use case for Received signal strength indicator (RSSI) based positioning is often locating a user with a personal device, usually a smartphone, which is able to receive RSSI from stationary devices, whose location is known. These stationary devices are often BLE beacons or Wi-Fi Access Points. One common approach for positioning is based on a fingerprinting method, which consists of two stages: offline and online stage. During the offline stage, RSSI values from the transmitting devices are recorded at several calibration points forming fingerprints for those locations. During the online stage, the user's current RSSI fingerprint is then compared to the offline fingerprints, and the best fitting location is selected as the user location. Fingerprinting based user positioning has already been tested with ActiveAhead luminaires by Gadicherla [4]. [5]

However, in the case of this thesis, the problem is reverse: the scanner location is known but the location of the stationary devices, or in this case, luminaires, are not. Furthermore, in this case the measured RSSI values are not available at the luminaire locations, but a user smartphone is used for RSSI scanning. Therefore, fingerprinting-based methods do not seem usable since they would require comparing the fingerprint received at the luminaire with the calibration fingerprints, and in this case, the luminaire fingerprint was not assumed to be available.

In addition to the user localization, another common use case for RSSI-based positioning is locating the nodes in wireless networks. This type of device localization is often performed with anchors, i.e., nodes with known positions used to locate the rest of the nodes [6]. However, the anchor-based methods also require the RSSI information between the anchor and their nearby nodes [7], and as stated previously, this information was not assumed to be available. Therefore, anchor-based methods did not seem to be of help for this thesis.

Trilateration utilizes the geometry of circles to locate an object with an unknown location, in this case a luminaire, based on the distances to known locations [7], in this case scan points. In the case of the device positioning, the distances to the known locations can be estimated based on the RSSI with a help of a path loss model [5]. It appeared that the described method could be applicable to the luminaire positioning problem and hence, it is more thoroughly explained in the following Sections 2.1.1 and 2.1.2.

The PIR triggers from the luminaires' PIR sensors were the second source of location information. However, there seemed to be no significant research done to the author's best knowledge on identifying the PIR sensors based on the known position of the triggers. The reverse problem of human position detection using a grid of PIR sensors with known locations has been researched, but is not directly relevant for this thesis.

2.1.1. RSSI-Based Distance Estimation

Received signal strength indicator (RSSI) is a measurement of power present in the received radio signal, indicating how much the signal is attenuated between the transmitter and the receiver. RSSI can be measured in milliwatts or decibels, but generally only its variations are of interest in the context of device positioning. RSSI is often quantized to integers which is the case also in Android BLE interface [8] which is later used in the thesis.

RSSI is inversely proportional to the distance in an empty space, and this property is utilized in RSSI-based distance estimation. This relation is commonly expressed with a log-distance path loss model

$$RSS = A - 10n \log_{10}(d/d_0), \tag{1}$$

where A is the received signal strength at d_0, n is a coefficient describing the attenuation properties of the environment and d is the distance between the transmitter and the receiver. Often d_0 is set to one meter. [9].

In general, the coefficient n increases in environments with more obstacles [10] and especially when there are obstacles between the transmitter and receiver [11]. Commonly used path loss exponents n with 2.4 GHz frequency band are [10],

- n=2 for free space,
- n=1.6 to 1.8 in building with line-of-sight (LOS) conditions and
- n=4 to 6 for obstructed building conditions.

Miranda et al. [10] have verified that these path loss exponent values seem to work also in practice. Nevertheless, they are always subjective to the current environment [12].

Equation 1 presents the ideal case for the log distance path loss estimation, but in reality, it is not as straightforward. Usually, there are obstacles in the signal propagation path in indoor spaces, which can introduce time-varying characteristics to the signal with several ways:

- Reflections can occur when the radio waves propagating through the space hit a surface larger than their wavelength and they are partially reflected and partially penetrate the surface. In the case where the surface material is a perfect conductor, the signal is reflected without an energy loss. [12]
- Diffractions can occur when there is an obstacle with sharp edges between the transmitter and the receiver producing secondary waves which bend around the obstacle. Thus, the radio signal has a non-zero strength in the shade of the obstacle. [11, 12]
- Scattering can occur when the radio waves propagating through the space hit a surface smaller or approximately equal to the wavelength. The reflected energy is spread to all directions. [11, 12]

Generally, determining which of these phenomena has the greatest impact on RSSI is not possible [12]. Human bodies also absorb 2.4 GHz frequency band signals significantly, the absorption occurring stronger closer to the transmitter, which makes

the amount of people in the room and the orientations of the users a factor in the signal propagation [13][14]. Even the indoor temperature and humidity [15] conditions as well as Wi-Fi scanning and network access [16] can have an effect on the measured RSSI. Furthermore, different smartphones [17][4] can have an effect on the measured RSSI. Also, in the context of the ActiveAhead, the luminaire casing can also affect on the RSSI [4].

In addition to the variation caused by the previously mentioned phenomena, BLE signal RSSI can vary even more than the measurement noise due to the use of three advertising channels and frequency dependent fading [16]. Therefore, smoothing or filtering the RSSI measurements is a necessity [16]. For this purpose, average and weighted filters are some easily implementable options [14]. Kalman filtering is also commonly used [6][9]. Having more RSSI measurements generally increases the accuracy but also prolongs the scanning duration, i.e., filtering is always a trade-off between speed and accuracy [14]. Another way for coping with the RSSI fluctuation is to introduce a second Bluetooth gateway but with a known position to measure the RSSI of the surrounding beacons [9].

Supervised learning with neural networks have also been suggested for RSSI-based distance estimation [9] but this approach requires labelled training data, which in this case would be the distances between the transmitters and the receivers with the corresponding RSSI measurements. Similarly, parameters n and A for a log distance path loss model could be optimized to fit the current signal propagation environment as well as possible. However, these types of approaches do not seem directly applicable. The luminaire positioning and identification is a one time effort, and when the luminaire identifiers are determined, the problem is already solved and there is no need for more accurate positioning anymore. It is possible to apply the gathered training data to other spaces, but this type of approach would probably not generalize well since the signal propagation environments are often unique.

2.1.2. Deriving the Luminaire Position from the Estimated Distances

Trilateration is a basic approach utilizing three or more overlapping circles to identify the position P [5] as visualized in Figure 2. Measuring $RSSI$ from a transmitter with an unknown location P at p_1 and at p_2 leads to the knowledge that P must locate either at P_4 or P_1. With the knowledge of the third distance d_3, $P(x, y)$ can be solved analytically since it satisfies the three equations:

$$\begin{aligned} (P_x - p_{1x})^2 + (P_y - p_{1y})^2 &= {d_1}^2 \\ (P_x - p_{2x})^2 + (P_y - p_{2y})^2 &= {d_2}^2 \\ (P_x - p_{3x})^2 + (P_y - p_{3y})^2 &= {d_3}^2 \end{aligned} \tag{2}$$

Due to the errors in RSSI-based distance estimation, the circles may not intersect at the same point making the equations unsolvable. Also, the analytical solution does not scale very well due to the need for exactly three scan points.

One way to mitigate these drawbacks is to approach trilateration as an optimization problem. In general, the goal in optimization is finding the best possible solution from

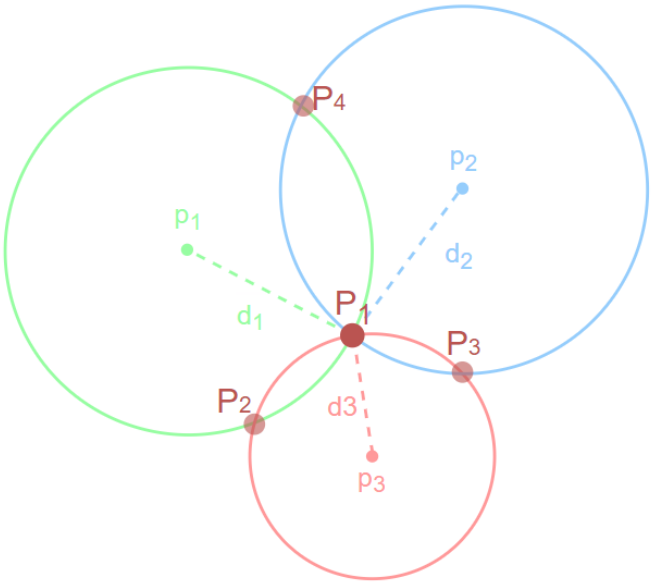

Figure 2. The principle behind ideal trilateration: d_1, d_2, d_3 represent the distances estimated from RSS attenuation from unknown location P to p_1, p_2 and p_3. P_1 represents the true location for P whereas P_2, P_3, P_4 are the other possible locations for P when knowing only the measurements from two points from p_1, p_2 and p_3.

a set of alternatives and possibly with given a set of constraints [18 p.1]. Finding the best possible solution is done either by minimizing or maximizing an objective function $f(x)$, which is in minimization often referred to as a loss function $L(x)$. The best possible solution is worked towards in an iterative manner by, improving a given initial guess, for example, based on the gradient of the objective function. For example, mean squared error (MSE) can be used to represent the loss function

$$L(x) = \frac{\sum_{n=1}^{N}[d_n - dist(P_{guess}, p_n)^2]}{N}, \tag{3}$$

where d_n is the estimated distance based on $RSSI$ between the nth scan point p_n and the transmitter location P, P_{guess} a guess for the transmitter location for each iteration, and N the total number of scan points. There are several optimization methods, such as least squares [14][9], that can be used for solving the optimization problem. Further comparison of the optimization algorithms is not in the scope of this thesis.

2.2. Lighting Control Prototype for Collaborative Spaces

The second goal of the thesis was to design and implement a lighting control prototype to a particular collaborative space, Business Kitchen, at the University of Oulu by utilizing the installed ActiveAhead luminaires and possibly other sensors and hardware if needed. Section 2.2.1 takes a look at some previously designed and implemented smart lighting systems to gain insight into how personal lighting control could be implemented in the Business Kitchen collaborative environment.

2.2.1. Related Smart Lighting Systems

ActiveTune[2] is a mobile application developed for ActiveAhead luminaires to enable lighting control for a particular luminaire or a group of luminaires. To adjust the intended luminaire(s), users need to scan a QR code which is usually placed beneath the luminaire(s). A graphical user interface (GUI) is used to control the lighting intensity and also temperature if the luminaire hardware supports temperature adjustments. In Business Kitchen, ActiveTune would work well when the desks are placed directly beneath a luminaire. However, generally this was not the case since the luminaire layout was designed to provide general lighting to the whole area, not task specific lighting to particular work desks. Furthermore, ActiveTune does not support luminaire sharing which could be useful especially in the case where there are luminaires located between users.

Zou et al. [19] have developed a lighting control approach named Winlight utilizing Wi-Fi based occupancy sensing. User positions were estimated using Wi-Fi Access Points (APs) with special firmware enabling listening to the Wi-Fi traffic of the users and at the same time capturing the RSSI values. Lighting levels were calculated based on the occupancy data according to a lighting control algorithm aiming to satisfy the lighting preference of each person while minimizing the energy consumption. In the case where there were multiple persons in the room, their preferences were averaged. Also, the developed hybrid mobile application enabled the brightness adjustment from a list of nearby luminaires. Users could also store luminaire presets which would be activated when entering the same zone where the luminaires were located. [19]

The developed Wi-Fi based occupancy detection was able to identify the correct zone from four equally divided zones in a 7m x 10m room by 98.66 %. Joining a Wi-Fi access point was mandatory for the system to work, but the APs also provided Internet access.[19]

A system proposed by Krioukov et al. [20] did not use any indoor positioning technologies but a web interface which could be used to select zones where users want to adjust the lighting. Also, QR codes with a direct link to the corresponding luminaire in the web interface were placed to the corresponding zones to ease the use. Timers with three hour duration were used to turn off the lighting. Campus credentials were used for authentication and recognizing potential system abusers. There was no automatic conflict resolution in place and the users were assumed to solve the potential conflicts by themselves. [20]

In addition to the QR codes, Near Field Communication (NFC) tags with unique identifiers have been utilized to detect the user presence and location by Petrushevski [21] in a work desk setting. The system enabled input of the users' lighting preferences with an Android application after touching a NFC tag. The preferences were then forwarded to a server module containing a space model with the luminaire and NFC tag position information. The server module was also responsible for sending control messages to the closest luminaires. Furthermore, the lighting output was adjusted by utilizing the information of the smartphone's illuminance sensor until the preferred lighting level was achieved.

[2]https://helvar.com/fi/activetune-app/

Chandrakar et al. [22] have also used NFC in their prototype for providing lighting profiling. In their approach, the locations where lighting was intended to be adjusted would be equipped with NFC readers and the different lighting preferences were indicated by NFC tags which users carried with them. The drawback with this approach is that the users would need to carry an additional NFC tag for each preference they had. On the positive side, the system enabled accessibility for everyone in the space since users did not need to have an application installed into a mobile device or even the device with them. The system was intended for home use and therefore did not have any type of conflict resolution. Comparison of the lighting systems is presented in Table 1.

Table 1. Comparison of the related lighting systems

Company / Research group	Occupancy detection	Control	User Interface	Conflict management	Authentication
Helvar Oy Ab, ActiveTune	BLE connection	Distributed	Mobile app	Left to users	BLE connection, possible to set a PIN code
Zou et al. [19]	Wi-Fi fingerprinting	Centralized	Hybrid mobile app	Preference average	Wi-Fi network, application credentials
Petrushevski [21]	NFC	Centralized	Mobile app	Preference average weighted by distance	-
Krikov et al. [20]	GUI, timeout	Centralized	Web app	Left to users	University credentials

3. BUSINESS KITCHEN INFRASTRUCTURE

The ActiveAhead smart lighting system utilized in this thesis had been installed to the Business Kitchen at the University of Oulu. Business Kitchen, presented in Figure 3, is a collaborative space containing several movable tables for studying or group work and also a stage for giving presentations.

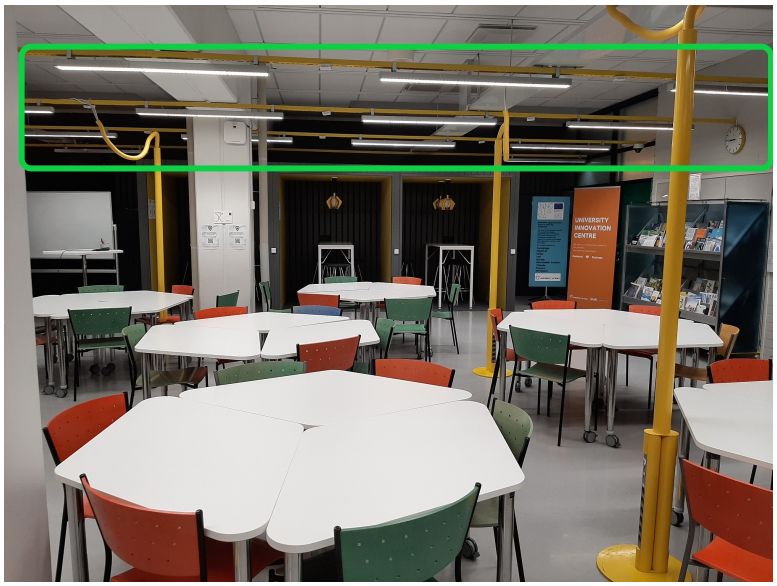

Figure 3. Business Kitchen. The ActiveAhead controlled Greenled luminaires are attached to the yellow beams (green).

3.1. ActiveAhead Luminaires

There are a total of 84 smart luminaires which were utilized in this thesis installed in Tellus at the University of Oulu Linnanmaa campus. Luminaires are the model of Omega 44W[3] manufactured by Greenled and controlled by ActiveAhead control units[4]. Each control unit is equipped with a sensor unit[5] containing a passive infrared (PIR) sensor to detect motion and an illuminance sensor. Together these sensors enable energy savings by turning off the lights when the space is not occupied and by adjusting the luminaire's artificial lighting output based on the variation of natural light during the day. Since PIR sensors are essential technology for this thesis, their general functionality is explained described in Section 3.1.1.

ActiveAhead control units are able to communicate with each other through a low-energy Bluetooth mesh network, explained in Section 3.1.2, and can learn the general routes people tend to walk based on the PIR triggers and pre-emptively light up. Furthermore, the luminaires in Tellus can be used as actuators through an interface which was kindly provided by the ActiveAhead manufacturer Helvar Oy Ab.

[3]https://greenled.com/lighting-products/product/omega-5/
[4]https://helvar.com/product/5605-activeahead-control-unit/
[5]https://helvar.com/product/active-sense-sensor/

Other technologies, such as ZigBee[6] and Wi-Fi[7], has also been utilized for the smart luminaire communication. For example, Philips Hue uses ZigBee[8] and LIFX[9] Wi-Fi as their underlying communication technologies, but since the existing ActiveAhead installation utilizes BLE Mesh, the other technologies are not explored further.

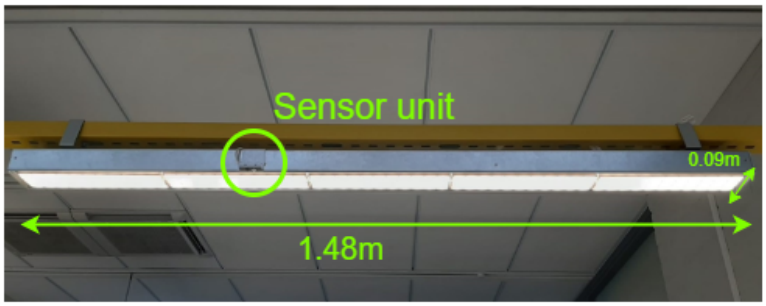

Figure 4. One of the smart luminaires in Tellus.

3.1.1. Passive Infrared Sensors

A passive infrared sensor (PIR) contains a sensing element made which generates an electric charge when exposed to infrared (IR) radiation at the electromagnetic spectrum. Usually PIR sensors are used to detect human motion, especially in security and energy management systems. Therefore, the sensing element must be capable of detecting far-infrared radiation from 4 to 20 μm which is the wavelength interval of the radiation emitted by humans. [23 p.267]

The sensing element in a passive infrared sensor is commonly made from a pyroelectric material and split into two halves which are wired up in a way that their signals cancel each other out [23 p.268-269]. Thus, the sensor causes a trigger only when either half detects either more (or less) IR radiation than the other half [24]. Therefore, only moving IR sources are detected, whereas the background IR radiation is nullified. In other words, people who remain stationary cannot be detected [25] which is often countered by setting timeouts in the context of lighting control.

The sensing elements by themselves can only cause triggers directly from the direction they are faced. Therefore, a lens, most commonly Fresnel lens, is needed to pinpoint the radiation from multiple directions to the two sensing halves making the detection area wider and circular [23 p.270]. Even though the detection area is made circular, it is good to note that it is not a perfect circle but consists of several smaller areas depending on the pattern of the lens. The detection diameter of the PIR sensors installed on the ActiveAhead control units is 8 meters at the ground level when installed at 3 meter height [26].

Single PIR sensors are capable only for detecting if there is someone present in the range of the sensor. However, when connected to a network of other PIR sensors partial

[6]https://zigbeealliance.org/
[7]https://www.wi-fi.org/discover-wi-fi
[8]https://www2.meethue.com/
[9]https://eu.lifx.com/

counting, localizing and tracking become possible with the accuracy depending on the number of nodes.[25]

3.1.2. Bluetooth Low Energy Mesh Network

Bluetooth low energy(BLE) is a communication technology operating on 2.4 GHz industrial, scientific and medical (ISM) band of radio spectrum, specifically on the area between 2402 MHz and 2480 MHz defined as part of Bluetooth 4.0 specification [27]. As its name implies, BLE is a variant version of Classic Bluetooth with lower power consumption having a data rate of 1 Mbps. Most modern smartphones, tablets and laptops support BLE, which has contributed making it one of the dominant technologies for Internet of Things (IoT) [28].

Since BLE channels are spaced with 2 MHz intervals, there are a total of 40 usable channels. The channels are utilized by the two modes of BLE communication: advertising and communication-oriented modes. Channels 37, 38 and 30 act as a medium for the advertising mode used for discovering other BLE devices, establishing connections and broadcasting information. While a device is broadcasting, other devices can scan the three channels one at a time to receive the information when the scanner is in the range of the broadcast. The remaining 37 channels are used for bidirectional communication between the connected devices. [29, 30, 28] Both of these modes can be used for implementing Bluetooth mesh, but the advertising mode has been chosen for Bluetooth Mesh Standard by the Bluetooth Special Interest Group (SIG) [28].

Bluetooth Mesh Standard enables many-to-many device communication by utilizing flooding principle which means every node in the network transmits to its neighbors. Since flooding can lead to scalability and robustness problems, a relay feature was implemented to the mesh standard meaning that only specific relay nodes are able to forward the messages by flooding. The standard also introduces time-to-live (TTL) fields and a relay cache which ensure that the messages are transmitted only when TTL is greater than 1 and the message has not gone through the same node before. BLE mesh also introduces proxy nodes enabling older BLE devices such as smartphones to be connected to the network. The proxy nodes also need to act as relay nodes so that the messages from the smartphone are forwarded into the network. [28]

3.2. Determining the True Positions of the Luminaires

The true positions of the luminaires were determined by measuring the distances of the PIR sensors between reference luminaires in x- and y-directions. The positions of the remaining luminaires were derived assuming that the distances between the luminaires were constant, which seemed to be the case with visual inspection. The method resulted to a positioning error of 0.6 cm for the outermost luminaire in the x-direction and 3.5 cm error in the y-direction for the outermost luminaire what could be measured. The luminaires used for measuring the error are circled with blue and red in Figure 5 for x- and y-directions respectively. The larger error to the y-direction is most likely due to the fact that the PIR sensor units were not locked in

place, whereas the x-direction was fixed since the luminaires were attached to existing beam infrastructure. The method for determining the error is not conclusive since all columns and rows of luminaires were not measured but considered acceptable as well as the error itself, since the true positions would be approximations also in the actual luminaire identification scenario. The luminaires were identified by manually flashing each luminaire by using ActiveAhead Mobile application[10] and recording the corresponding identifier.

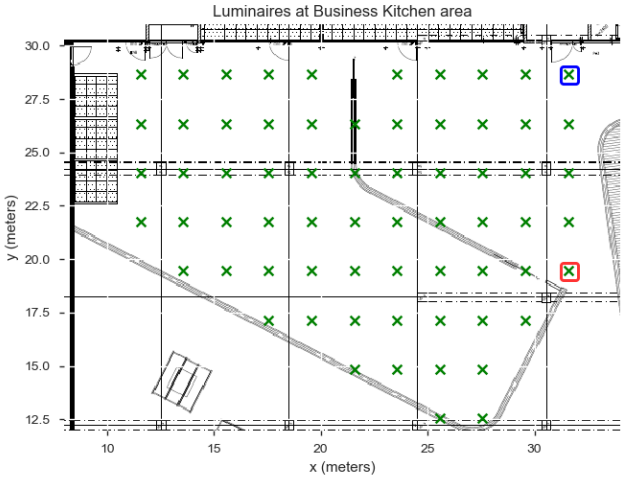

Figure 5. The positions of the luminaires at Tellus Business Kitchen. The Green crosses represent the determined true positions of the luminaires' PIR sensors. The distance between luminaires is 2.0 meters to x-direction and 2.3 meters to y-direction.

[10]https://helvar.com/product/activeahead-mobile-app/

4. SMART LUMINAIRE POSITIONING

This chapter investigates how the smart luminaire positioning can be performed by the information from PIR sensor triggers and RSSI broadcasted by the luminaires.

The first step was to develop an application for recording user position, RSSI values and PIR sensor triggers based on the problem definition, see Section 1.1. The developed application was then used to record *PIR EDA dataset* containing around 80 minutes of walking in Business Kitchen. It was observed that PIR sensor triggers seem to form clusters around the luminaire placeholders leading to a development and evaluation of a centroid-based location estimation. The method provided 1.69 meter mean error at around 10 minutes with *PIR EDA dataset*, see Figure 15 for more detailed results. Furthermore, it was reasoned that the developed centroid method is highly dependent on the performed walking pattern, thus another dataset, *PIR optimal dataset*, was gathered to observe if the method performs better with optimal walking which indeed seemed to be the case: the method achieved a mean error of 0.47 meters in 10 minutes with *PIR optimal dataset*, see Section 4.3.2.1 for more detailed results.

For the RSSI, 9 scan points with one minute duration were recorded, referred as *RSSI dataset*. The RSSI-based method consisted of log-distance path loss distance estimation and mean squared error (MSE) based optimization providing a 3.12 meter mean error with path loss exponent of $n = 1{,}6$ at the maximum of 9 scan points. The worse performance of the RSSI-based method compared to the PIR-based method was to be expected due to the time-varying characteristics of the BLE RSSI indoors. Nevertheless, RSSI can provide a fast way of getting approximates of the luminaire positions in the case where the accuracy requirement can be relaxed. RSSI and PIR-based methods are further compared in Section 4.5.1.

4.1. Application for Data Gathering

The following requirements were defined based on the problem definition presented in Section 1.1:

- The user needs to be able to input the start and the end points for a walk
- The user needs to be able to start and end BLE scanning
- The user needs to be able to estimate his/her position in the space
- BLE RSSI values need to be timestamped and recorded
- PIR sensor triggers need to be timestamped and recorded
- The start and end points of the walk need to be timestamped and recorded

An Android mobile application was developed based on these requirements. Google Maps software development kit (SDK)[11] was used to provide a floorplan as a background image and markers to indicate the current position on the floorplan. Android Bluetooth API[12] was used for scanning the BLE advertisement packets broadcasted by the luminaires. The Android BLE scanning interface requires the user to enable the device location and Bluetooth during scanning.

[11] https://developers.google.com/maps/documentation/android-sdk/intro
[12] https://developer.android.com/guide/topics/connectivity/bluetooth

The intended flow for the data gathering process is presented in Figure 7 and the GUI states for performing walks can be seen in Figure 6. The green and red markers indicate the start and end points of a walk. The user is only allowed to walk between the start walk and end walk events to maintain the knowledge of the user position at all times. During a scan, the start (green) marker is placed automatically and cannot be modified by the user since it is assumed that a new walk will always start from the end point of the previous walk. If the user wants to continue the luminaire positioning from a location other than where the previous walk ended, it is possible to end the scan, move to the new location and start the process again. Also, dragging the start and end point markers during a walk is disabled to avoid missclicks.

During prototyping, it was noticed that walks can go wrong by several ways: the user might forget to press the "End walk"-button precisely when having finished the walk, or the user might notice that she walked further than intended, both of which lead to an error in the user position. Therefore, a functionality to discard previous walks was implemented by adding a ”Discard”-button which writes a discard event to the log file enabling the removal of the failed walks during the preprocessing of data.

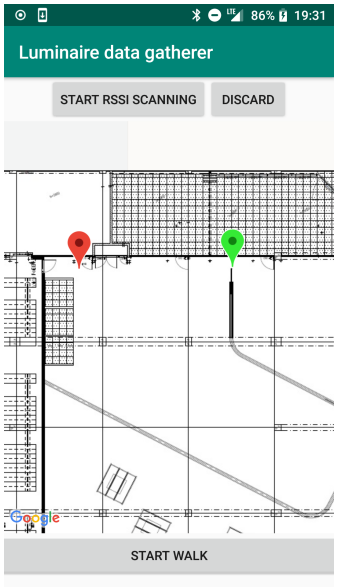

(a) The initial state before starting scan. User has moved to the start point (green marker) and prepares to walk to the end point (red marker).

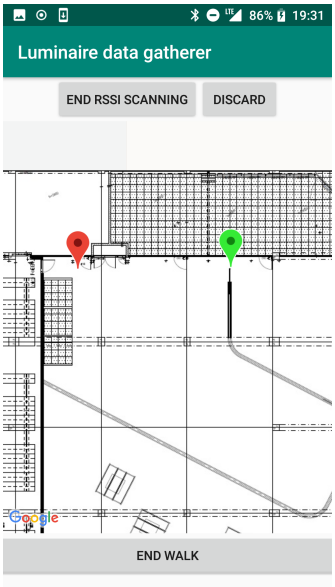

(b) Performing the walk from the the start point (green marker) to the end point (red marker).

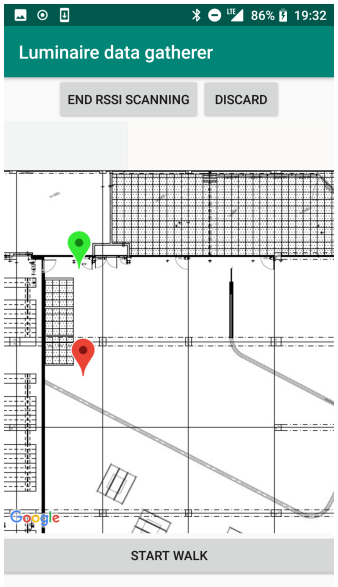

(c) Placing an end point for the next walk.

Figure 6. GUI states for performing walks.

Timestamps for user location events, i.e., when walks and scans started and ended, are recorded with the location coordinates. Also, the RSSI values are stored with the corresponding luminaire identifiers. The generated data is saved to a log file for which the device storage permission is required.

Helvar Oy Ab provided an external device for connecting to the luminaire Mesh Network and record the PIR sensor triggers during the scan. The triggers were recorded as binary data (on/off) when any of the triggering sensors registered movement. The

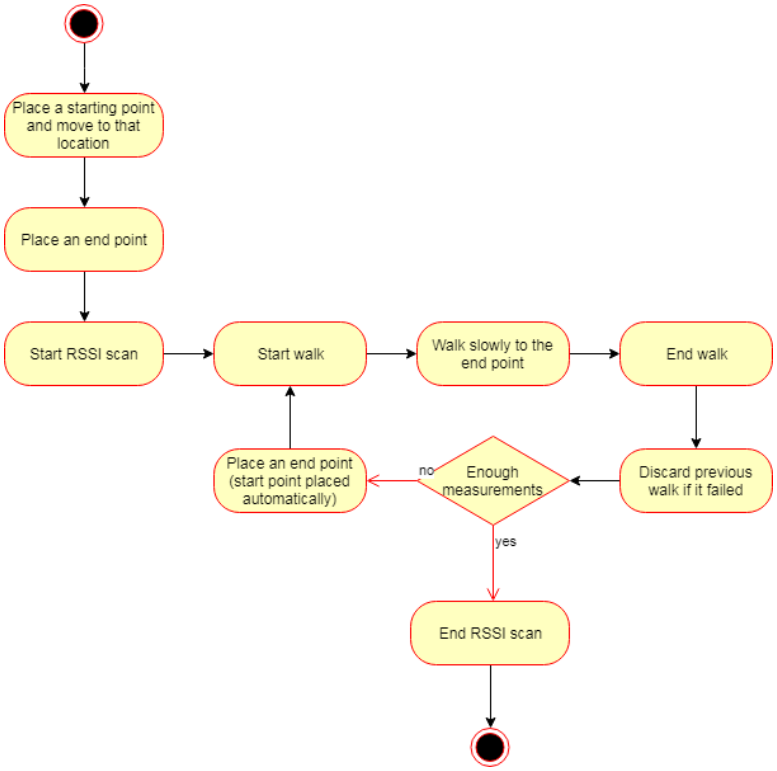

Figure 7. The steps for data gathering process using the application.

device supported a serial interface, thus a Python script was developed using Pyserial[13] module to timestamp each incoming PIR trigger. The triggers were then recorded to a log file so that the triggers could be later matched with the user location.

4.2. Data Preprocessing

The preprocessing of the gathered PIR triggers and RSSI values consisted of the following steps:

1. Parsing the log file produced by the data gathering application,
2. discarding failed walks,
3. converting the coordinates from Google Maps' latitude longitude to meters since the width, height and the position of the floorplan on Google Maps were known,
4. estimating the walking speed of the user assuming that the speed was constant during each walk,
5. estimating the position of the user for each received PIR trigger or RSSI value assuming constant walking speed,
6. calculating the direction where the user was walking for each data point based on the walk start and end points and
7. excluding PIR triggers before and after scans.

[13] https://pypi.org/project/pyserial/

A sample of the preprocessed data can be seen in Figure 8. Preprocessing was conducted using Python 3.6[14] and Pandas data analysis library for Python[15].

	Id	Rssi	Timestamp_unix	Y	X	Walking	Walk	Direction	Speed
95	D4C0	-89	1564853569404	25.5	11.22	True	0	180.14	0.78
96	D508	-97	1564853569447	25.46	11.22	True	0	180.14	0.78
97	D389	-83	1564853569466	25.45	11.22	True	0	180.14	0.78
98	DEA4	-83	1564853569496	25.43	11.22	True	0	180.14	0.78
99	D387	-97	1564853569518	25.41	11.22	True	0	180.14	0.78
100	D3B1	-77	1564853569656	25.3	11.22	True	0	180.14	0.78
101	D446	-91	1564853570140	24.93	11.21	True	0	180.14	0.78
102	D4E7	-84	1564853570187	24.89	11.21	True	0	180.14	0.78
103	D3B9	-76	1564853570198	24.88	11.21	True	0	180.14	0.78
104	CFB0	-88	1564853570212	24.87	11.21	True	0	180.14	0.78
105	D4B1	-93	1564853570252	24.84	11.21	True	0	180.14	0.78
106	DEBD	-96	1564853570278	24.82	11.21	True	0	180.14	0.78
107	CF89	-96	1564853570306	24.8	11.21	True	0	180.14	0.78
108	D3BA	-90	1564853570326	24.78	11.21	True	0	180.14	0.78
109	DCED	-93	1564853570341	24.77	11.21	True	0	180.14	0.78
110	D4F4	-86	1564853570366	24.75	11.21	True	0	180.14	0.78
111	D396	-83	1564853570387	24.74	11.21	True	0	180.14	0.78
112	D4FE	-88	1564853570414	24.71	11.21	True	0	180.14	0.78
113	D1C7	-89	1564853570431	24.7	11.21	True	0	180.14	0.78
114	CED2	-87	1564853570463	24.68	11.21	True	0	180.14	0.78

Figure 8. A slice of preprocessed RSSI data.

4.3. PIR-Based Method for Luminaire Positioning

The data gathering application presented in Section 4.1 was used for gathering two datasets, *PIR EDA dataset* and *PIR optimal dataset*, in Business Kitchen. For both datasets it was made sure that no one else was present in the space during the data gathering to avoid PIR sensor triggers from anyone else but the data gatherer. The data gathering was performed with Samsung Galaxy S8 smartphone with Android 7.0 operating system. The Python script for PIR recording was started on a laptop and left running during the data gathering process. The triggers from ActiveAhead PIR sensors were collected separately with a laptop by running the Python script.

4.3.1. PIR EDA Dataset

The goal of *PIR EDA dataset* was to gain a better understandin of the data with Explorative Data Analysis (EDA). Especially how the PIR sensors trigger while walking, and what patterns can be observed in the data afterwards, were areas of interest. The tables and other pieces of furniture restricted the possible walking paths since the walks needed to be direct from the start to the end point. Estimating the start and end points from the floorplan during data gathering was easier near to known landmarks, such as pillars and beams, that also affected the walk paths. The performed

[14]https://www.Python.org/
[15]https://pandas.pydata.org/

walks are visualized in 9. *PIR EDA dataset* was gathered during three scans and later combined containing 189 walks that took 80.5 minutes to be recorded.

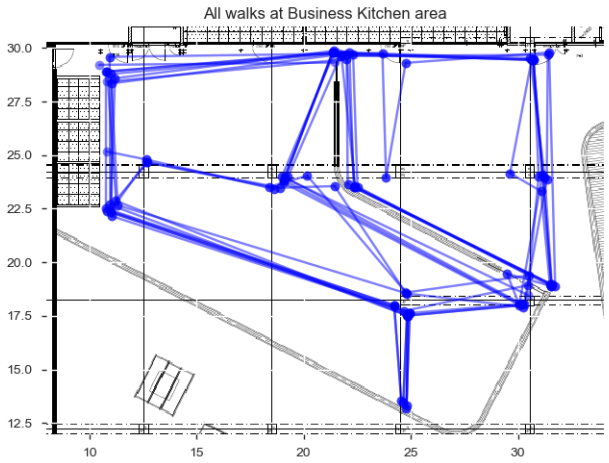

Figure 9. All walk paths in *PIR EDA dataset*. Due to the obstacles, such as furniture, chairs and tables, it was not possible to perform walks covering the whole space.

4.3.1.1. PIR Explorative Data Analysis (EDA)

The PIR sensors have a manufacturer announced range of 4 meters at 3 meter height [26]. In the case of Business Kitchen, the luminaires were placed at 2.6 meter height measured from the floor level which should make the range somewhat smaller. The detection range of the sensors was also inspected for *PIR EDA dataset* by calculating the distances between each trigger and the corresponding luminaire. The resulting distribution is presented in Figure 10a.

According to the Figure 10, 89% of the sensors trigger when the data gatherer was performing walks. The remaining 11% of the sensors trigger between the walks when the data gatherer was placing an end point for the next walk thereby trying to stand still. The movement during this phase could be caused from turning to the direction for the next walk or just by slightly moving in place. It is also possible that the data gatherer could have also pressed the "End walk" button slightly too soon. In any case, it seems that not causing sensors to trigger by trying not to move between the walks is very difficult or outright impossible.

The Figure 10 can also be interpreted in a way that if the distance between the luminaires is at least 4.57 meters, simply identifying the nearest placeholder as the trigger source results to a correct luminaire identification with 95% accuracy. Also, comparing the 95th percentile, i.e., 4.57 m, to the announced PIR detection range of 4 m indicates that there are errors present. Some of the possible sources of error are

1. the user's estimation of his/her position on the floorplan $E_{floorplan}$,
2. the derivation of the user position during a walk assuming constant speed and a straight walking line $E_{nonconstantspeed}$,

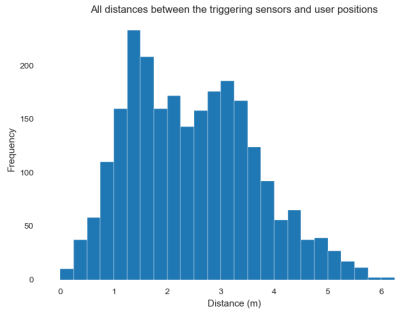

(a) The PIR histogram with all triggers, 2450 in total. 5% and 95% of the distances fall below 0.80 and 4.57 meters respectively. μ = 2.46 m, σ = 1.17m

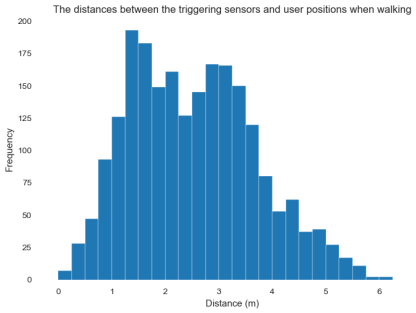

(b) The PIR histogram of the triggers when the data gatherer was walking, 2192 in total. 5% and 95% of the distances fall below 0.82 and 4.64 meters respectively. μ = 2.53 m, σ = 1.17m

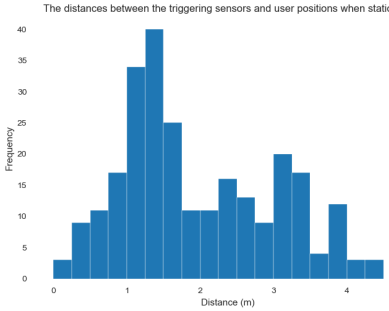

(c) The PIR histogram of the triggers when the the data gatherer was being stationary, 258 in total. 5% and 95% of the distances fall below 0.53 and 3.87 meters respectively. μ = 1.96 m, σ = 1.04m

Figure 10. The distances between the triggering PIR sensors to the user positions at the time when the sensor triggered. In the histogram the distances are divided to 0.25 m buckets.

3. PIR sensor detection pattern E_{PIR},
4. placeholder positioning error $E_{placeholder}$,
5. the delay of receiving the triggers from the luminaire network and registering them with the Python script E_{delay}.

$E_{floorplan}$ depends on factors such as the amount landmarks on the floorplan, the quality of the floorplan, the data gatherer's focus when positioning the start and end points for the walks and failing to indicate the start or end of the walks with the UI button at the right time. $E_{nonconstantspeed}$ is only present during walks. E_{PIR} is caused by the fact that the PIR sensor detection pattern is not a perfect circle but is formed from several areas, see Section 3.1.1. $E_{placeholder}$ has already been determined to be in a scale of a couple centimeters in Section 3.2. E_{delay} was not inspected further but assumed to be rather small compared to the other sources of error. Without further experiments, it was not possible to quantify the errors further.

The recorded PIR triggers were also plotted to better understand the patterns in the data. It was noticed that the triggers can form clusters around the sensor, of which an

example can be seen in Figure 11a. There were also cases when the clusters did not indicate the true position of the source luminaire, as can be seen in Figure 11b. The limited walking paths were most likely the reason for this behavior since the triggers can only be positioned to the walking paths. In the case of Figure 11b, for example, the walks in the dataset intersected only one side of the possible sensor trigger area.

Figure 12 represents the recorded triggers and the corresponding luminaire sensors for one of the performed walks. Generally, the luminaire sensors seemed to trigger when the data gatherer was walking towards or perpendicular to the sensors, but also triggers behind the data gatherer were observed during the start of the walks.

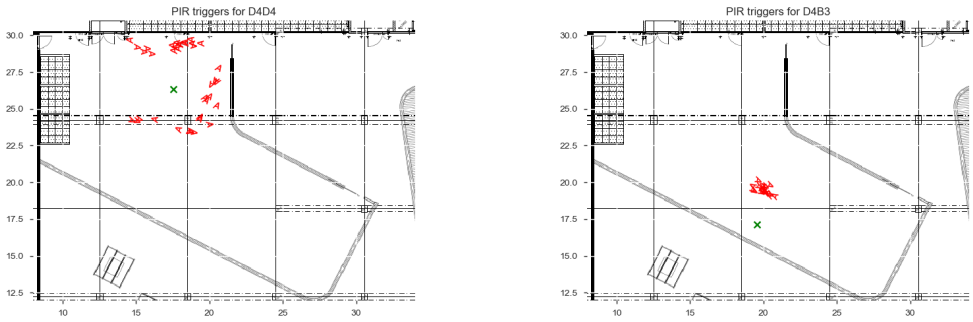

(a) All PIR triggers for the luminaire with id D4D4. An example of clustering.

(b) All PIR triggers for the luminaire with id D4B3. An example when the triggers did not seem to form a cluster.

Figure 11. Two examples of PIR triggers per luminaire sensor. The green cross represents the luminaire sensor location, whereas the letter "A" is used to indicate the direction of the walk when the PIR sensor was triggered. Upwards facing A indicates a walk from bottom to top.

4.3.1.2. PIR Method - Centroid-based ranking algorithm

During EDA, it was discovered that some of the PIR sensors seemed to produce clusters of triggers around them. Therefore, estimating luminaire positions as the centroid of the trigger cluster, i.e., the average of the x- and y-coordinates, seemed a viable option. The developed algorithm consisted of two steps: forming a candidate for every placeholder by calculating the distances between every PIR cluster centroid described in Algorithm 1, and placing the estimates to placeholders described in Algorithm 2. Basically, the algorithm can be seen as fitting each centroid of the PIR trigger to each luminaire placeholder and selecting the best candidate as the luminaire identifier.

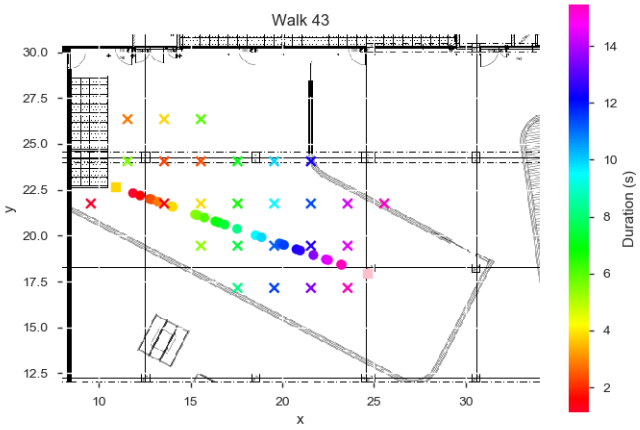

Figure 12. The PIR triggers for the walk 43 visualized. Yellow and pink squares indicate the start and end points of the walk respectively. The points show the estimated trigger location, whereas the crosses with the same color represent the PIR sensors causing the trigger. Colors also indicate the duration of the walk.

Algorithm 1. Form the candidate identifiers for the placeholder, i.e., calculating the distance between the PIR centroid and the placeholder for every luminaire sensor that has detected movement.

```
1  def form_candidates(placeholder, pir_triggers):
       Result: luminaire identifier candidates for the placeholder
2      candidates = []
3      for id in unique_ids_in_pir_triggers:
4          triggers_for_id = pir_triggers.filter(id)
5          x_coords = []
6          y_coords = []
7          for trigger in triggers_for_id:
8              x_coords.append(trigger.x)
9              y_coords.append(trigger.y)
10         centroid = Coordinate(calc_average(x_coords),
             calc_average(y_coords))
11         d = calc_euclidean_distance(centroid, placeholder)
12         candidates.append(Candidate(d, id))
13     return candidates
```

Algorithm 2. Map the candidate identifiers to the placeholders.

```
Input  : placeholders, pir_triggers
Output: identified_placeholders
placeholders_with_candidates = []
for placeholder in placeholders:
    candidates = form_candidates(placeholder, pir_triggers)
    candidates.sort(key = distance)
    placeholder_with_candidates = PlaceholderWithCandidates(
        distance_to_nearest_candidate = candidates[0].distance,
        placeholder = placeholder,
        candidates = candidates
    )
    placeholders_with_candidates.append(placeholder_with_candidates)

placeholders_with_candidates.sort(key =
  "distance_to_nearest_candidate")
identified_placeholders = {}
for placeholder_with_candidates in placeholders_with_candidates:
    placeholder = placeholder_with_candidates.placeholder
    for candidate in placeholder_with_candidates.candidates:
        if identified_placeholders.get(candidate.id) is not None:
            continue
        e[candidate.id] = placeholder
        break
```

For the centroid method to be effective, a particular luminaire needs to be approached at least from two opposite directions, $D1$ and $D2$. Assuming the sensor trigger range is identical to both $D1$ and $D2$, and the walks are performed from both of these directions, the centroid of the two triggers is located at the true position of the luminaire. Performing one more walk (third in total) from $D1$, throws off the estimate, whereas performing the fourth walk from $D2$ balances the estimation again. With the previous reasoning, the algorithm should produce better results when the number of walks is even. Furthermore, the error from odd walks should decrease when the amount of walks is increased since the unbalanced odd walks have less weight in the centroid calculation due to the higher number of walks in total.

The easiest way to achieve identical trigger range for the sensor from $D1$ and $D2$ is to make them trigger as far away as possible, i.e., to approach them behind the trigger range. In practice, it is not always possible. In some cases, the luminaires may be placed near a wall or some other obstacle, which makes it impossible to start a walk outside the luminaire maximum trigger range breaking the symmetry and producing an error to the centroid estimation. This situation is illustrated in Figure 13 with the luminaire $L3$.

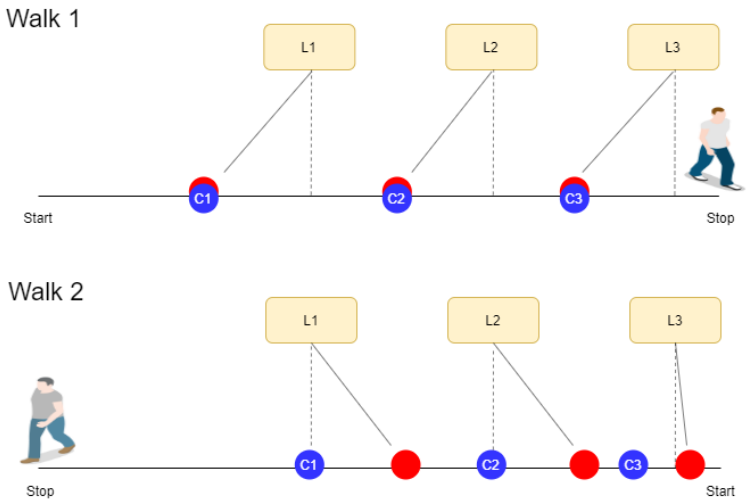

Figure 13. Calculating the centroids $C1$, $C2$ and $C3$ for luminaires $L1$, $L2$, and $L3$ respectively from the two walks. Red points represent the trigger locations and blue points the centroid of the triggers for a given luminaire. Since the first walk ends and the second walk starts under $L3$, $C3$ is not placed directly under $L3$. $L1$ and $L2$ are positioned correctly.

4.3.1.3. Evaluation

Two types of metrics were used to measure the performance of the algorithm presented in Section 4.3.1.2: mean error and accuracies for three different ranges. Mean error indicates the average distance between the estimated and the true positions of the luminaires. Accuracy metrics show how many of the luminaires were predicted to correctly locate within a given range. For example, having a $range_0$ accuracy of 20% means that 20% of the luminaires were placed exactly at their true locations and a $range_1$ accuracy 80% means that 80% of the luminaires were placed at least one placeholder away from its correct position. The three ranges used for accuracy are visualized in Figure 14. The mean error was calculated before mapping the identifiers to the placeholders, whereas the accuracy metrics were calculated after the mapping phase.

Information gain for a walk

$$I_{walk} = \sum_{n=1}^{N_{id}} \sum_{n=1}^{N_{triggers}} d(PIR_{latest}, PIR_{nearest}), \tag{4}$$

was also calculated for each walk and identifier by summing the distances between the most recent trigger to its nearest trigger to indicate how much new information had been gained from the walk. Simply presenting the new information with the walk index was not considered sufficient since the amount of PIR triggers per walk varied. The information gain for discovering a new sensor was set to the *PIR EDA dataset* mean trigger range of 2.46 m.

Figure 15 presents the results of the centroid algorithm, presented in Section 4.3.1.2, for *PIR EDA dataset*. Each point in the figure indicates the end of a walk, thus

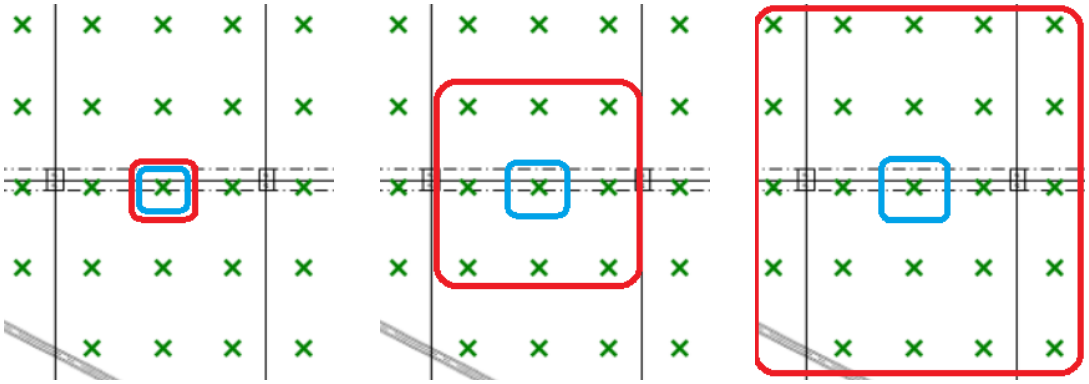

(a) $range_0$ (b) $range_1$ (c) $range_2$

Figure 14. The ranges for accuracy metrics visualized. The red circle shows all the luminaires labelled as correct when calculating the performance for a given metric. The true position of the luminaire is circled with blue.

containing the triggers during planning the walk when standing still and the triggers from the actual walk. There were three luminaires that did not cause any triggers, therefore those luminaires were excluded from the performance evaluation. The accuracy metrics were calculated by comparing the correctly identified luminaires to all luminaires in the space.

The mean error (Figure 15a) declines until 1.5 m error is achieved at around 60 walks; the following walks decrease the mean error only slightly. Small fluctuations in the mean error can be seen especially between the 10th and 60th walks, which can be caused by the imbalanced number of walks and asymmetrical trigger deviation around the sensors as seen, for example, in Figure 11b. At 10 minute mark a mean error of 1.69 was achieved with *PIR optimal dataset*.

The exact accuracy, or $range_0$ (Figure 15b), produces a more fluctuating curve compared to the mean error, but increasing the amount of walks generally leads to better $range_0$ accuracy. The more detailed results for *PIR EDA dataset* are presented in the Appendix 1.

4.3.2. Optimal Walking

Earlier in this thesis, see Section 4.3.1.2, it was reasoned that the performance of the centroid algorithm should increase when the data gatherer performs the walks optimally, i.e., starts the walks in a way that there is enough distance to the nearest PIR sensor so that the sensor is triggered from the maximum range. If the walks were performed in this manner, the luminaire identification time should decrease since only two triggers from opposite directions would be needed for a good estimate. The walks in *PIR EDA dataset* were not performed optimally since the layout of the luminaires and the space did not allow performing optimal walks. Therefore, a row of luminaires was picked to test if the performance of the centroid algorithm indeed increases with the optimal walks. This *PIR optimal dataset* dataset consisted of 36 walks and approximately 20 minutes of data gathering. The luminaires included in the dataset can be seen in Figure 16. The same setup was used to gather the dataset as

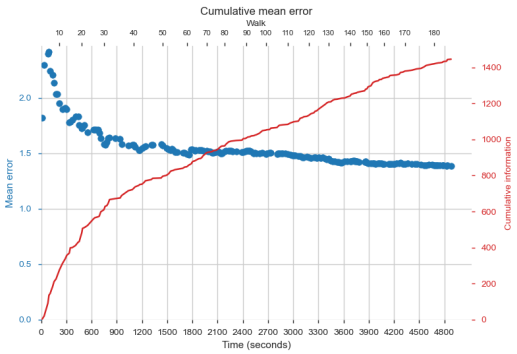

(a) Mean error

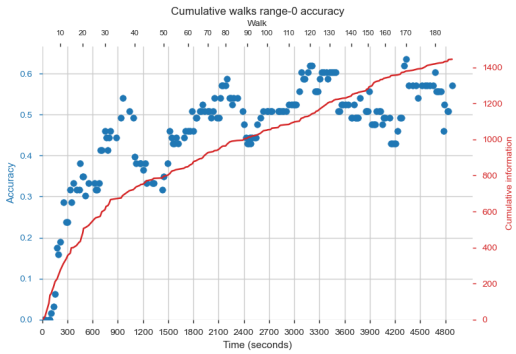

(b) $range_0$

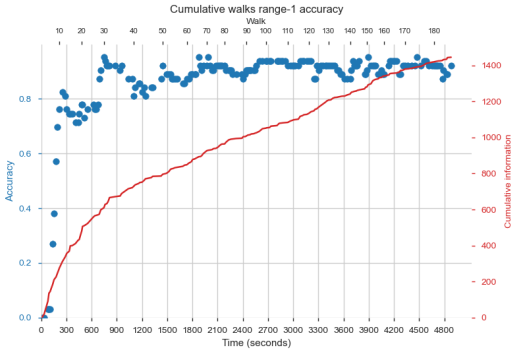

(c) $range_1$

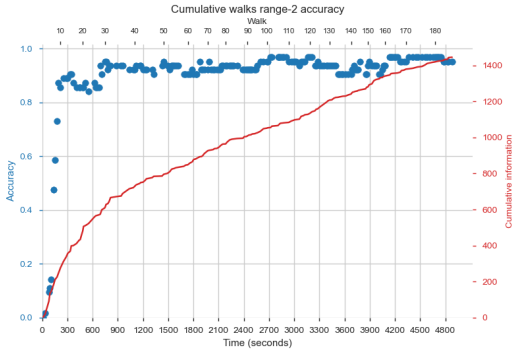

(d) $range_2$

Figure 15. Centroid algorithm performance for *PIR EDA dataset*.

with *PIR EDA dataset*, and the walking speed was attempted to be maintained constant during the walks. As can be seen in Figure 16, the walks were also attempted to be performed in straight lines directly under the PIR sensors as well as possible.

The mean distance between the user positions and the triggering sensors in *PIR optimal dataset* seems to be considerably higher than in *PIR EDA dataset*, which makes sense since the scenario attempted to trigger the sensors at maximum trigger distance at all times since none of the walks ended underneath the luminaires. Also, all triggers were caused during the walks, and therefore, only one distance histogram was plotted in Figure 17 in comparison to the three figures with *PIR EDA dataset*.

4.3.2.1. Evaluation

Figure 18 presents the results cumulatively for the centroid algorithm with *PIR optimal dataset*, i.e, the second plotted mean error in the figure contains the data from the first and second walk and so forth. All the six luminaires were discovered already during the first walk, and therefore, it did not matter if the accuracy was calculated by comparing the correctly identified luminaires to the discovered or total amount of luminaires.

The mean error (Figure 18a) seems to validate the reasoning presented in Section 4.3.1.2: The first walk produces an error comparable to the mean trigger range of 5.444 m, but the second walk decreases the mean error close to zero. The following even walks also seem to give better results in comparison to the adjacent odd walks.

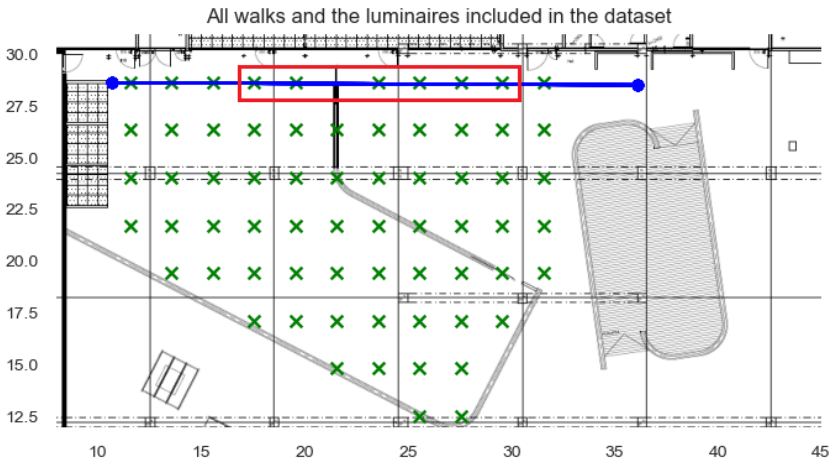

Figure 16. The 6 luminaires circled in red used for the *PIR optimal dataset*. The triggers from the rest of the luminaires were excluded. Walks that were performed are shown in blue lines.

Even walks do not seem to produce better results over time; in fact, the mean error seems to slightly increase, whereas the accuracy with the odd walks increases over time as predicted. The information gained from the walks after the second walk does not seem to increase considerably, which also indicates that the following walks provide a decreasing value. The mean error of 0.31 m is achieved at 5 minutes and 0.47 m in ten minutes when only considering even walks since it can be assumed beforehand that the even walks lead to better results.

The exact accuracy, or $range_0$ (Figure 18b), produced 100% accuracy already with the second walk and with the rest of the walks after the sixth walk. The method was able to identify only one luminaire correctly with the imbalanced third and fifth walks, again aligning with the predictions. The second walk was completed and 100% accuracy achieved at around one minute, but walking the same path repeatedly made the path planning slightly faster compared to the *PIR EDA dataset* since the application automatically swapped the start and end points of the walks and the data gatherer did not have to plan for the next walk.

4.4. RSSI-Based Method for Luminaire Positioning

The ActiveAhead luminaires form a Bluetooth Low Energy Mesh network and therefore occasionally broadcast BLE advertisements. These advertisements can be captured with any device supporting Bluetooth Low Energy also containing a RSS value indicating the distance to the advertiser. In general, higher RSS values indicate that the advertiser, in this case the luminaire, is closer. The goal of this section was

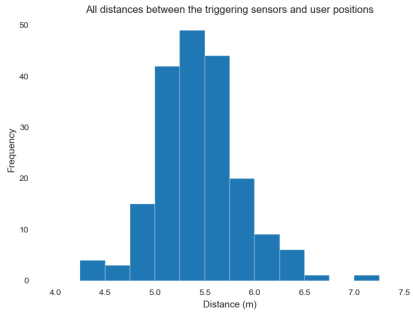

(a) The PIR histogram with all triggers, 194 in total. 5% and 95% of the distances fall below 4.80 and 6.17 meters respectively. μ = 5.44 m, σ = 0.42 m

Figure 17. The distances between the triggering PIR sensors and the user positions at the time when the sensor triggered with *PIR optimal dataset*. All the triggers were caused while walking. The distances are divided to 0.25 m buckets.

to choose a method to utilize the RSS information and evaluate its performance in identifying the luminaire in Business Kitchen.

4.4.1. The Chosen RSSI Method

Since the requirement was to capture the advertisements specifically with a smartphone, anchor-based methods were out of the question since they would require the RSSI received at the luminaire. Similarly, fingerprinting-based methods were also excluded since the fingerprints at the luminaire locations were not available. Based on the previous reasoning, a simple log path-loss model was chosen for estimating the distance from the RSSI. Mean filtering was used smooth the RSSI fluctuations. The distances between the scan points and the advertising luminaires were also converted to match the same two dimensional coordinate system as the luminaires to take account the fact that the signal propagation is spherical. This conversion was done with the Pythagorean theorem by using the height from the luminaires to the approximate smartphone height. The estimate for the luminaire position was found by minimizing the mean squared distance from the location estimate to the scan points by utilizing a SciPy implementation of Nelder-Mead[16] optimization algorithm. The average of the scan point coordinates was used as an initial guess for the optimization algorithm.

To identify the luminaires, luminaire candidate identifiers were formed for every placeholder by calculating the distances between the placeholder and the estimated luminaire position as presented in Algorithm 3. The best fitting candidates were placed to the placeholders similarly to the PIR-based identification by using 2. In other words, only the first step, i.e., the luminaire location estimation was different in the RSSI-based identification.

[16]https://docs.scipy.org/doc/scipy/reference/generated/scipy.optimize.minimize.html

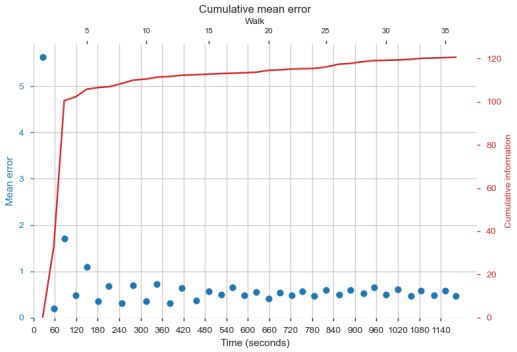

(a) Mean error

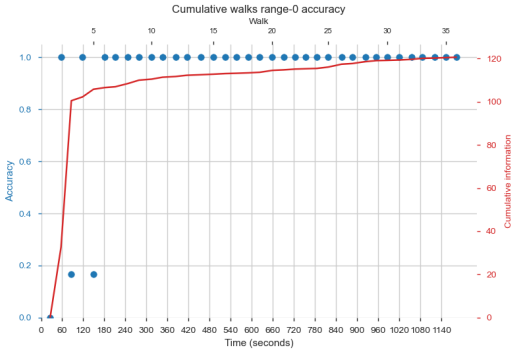

(b) $range_0$

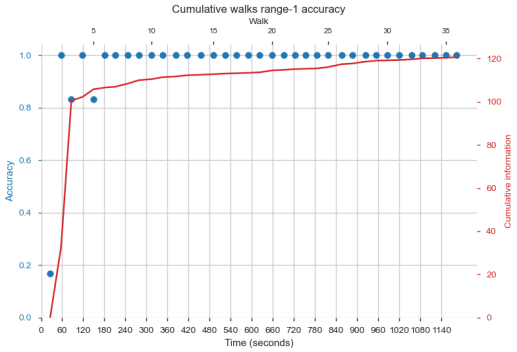

(c) $range_1$

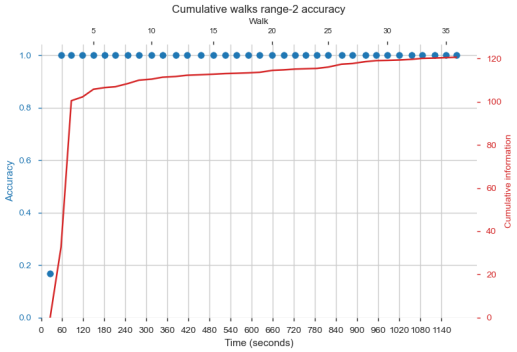

(d) $range_2$

Figure 18. Centroid algorithm performance for *PIR optimal dataset*.

Algorithm 3. Form the candidate identifiers for the placeholder with RSSI-based position estimation.

```
1  def form_candidates(placeholder, rssi_values, scan_points):
       Result: luminaire identifier candidates for the placeholder
2      candidates = []
3      distance_estimates = []
4      for scan_point in scan_points:
5          for id in scan_point.ids:
6              rssi_values_for_id_at_scan_point =
                rssi_values.filter(scan_point, id)
7              smoothed_rssi_value =
                smooth_rssi(rssi_values_for_id_at_scan_point)
8              d = convert_rssi_to_distance(smoothed_rssi_value)
9              d = convert_from_3D_to_2D(d)
10             distance_estimates.append([scan_point, id, d])
11     for placeholder in placeholders:
12         distance_estimates_for_id =
            distance_estimates.filter(scan_point, placeholder.id)
           scan_points_for_id = scan_points.filter(placeholder.id)
13         estimate_coord = optimize_location(scan_points_for_id,
            distance_estimates_for_id)
14         d = calc_euclidean_distance(estimate_coord, placeholder)
15         candidates.append(Candidate(d, placeholder.id))
16     return candidates
```

4.4.2. Log-Distance Path Loss Model Parameters

The log-distance path-loss distance estimation, which was presented in Equation 1, required measuring a calibration RSSI, A, from a known distance to the transmitter. To determine this calibration value, the RSSI was measured in Business Kitchen for three distinct luminaires by placing a Samsung Galaxy S8 smartphone one meter away from the transmitter with a help of a camera stand. The resulting RSSI for one of these luminaires, $C1$, can be seen in Figure 19, and the minimum, maximum and mean RSSI of these three luminaires in Table 2. The average of the RSSI means for $C1$, $C2$ and $C3$ (-74.722) was selected as the calibration RSSI, A.

With all three luminaires, it was noticed that the RSSI behaved in a relatively periodic manner, which was probably caused by the fluctuating power levels of BLE advertising and it has been seen in other studies [16][9] as well. In the case of $C1$, the first period seems to be completed at around 20 seconds, while the following cycles seem to be more difficult to distinguish. The observed periodic nature of the RSSI indicates that the scans need to contain at least one full period to be able to capture the true RSSI characteristics at a scan point.

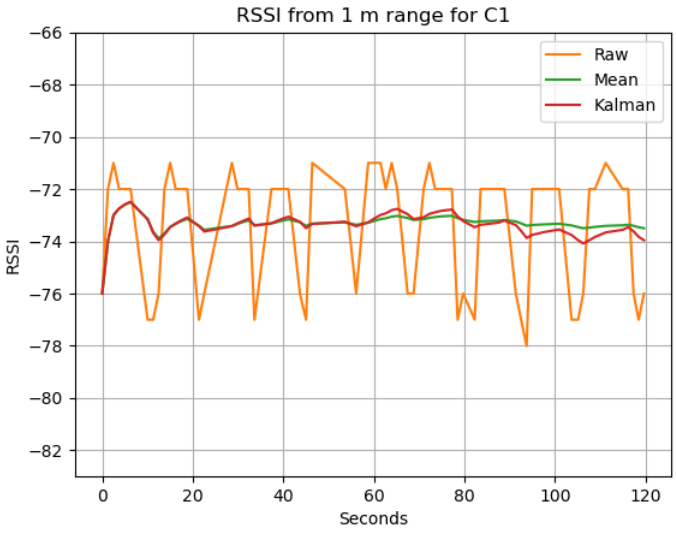

Figure 19. RSSI for luminaire $C1$ for two minutes.

Table 2. Calibration results

Luminaire	Min	Max	Mean	Count
C1	-82	-70	-75.031	65
C2	-81	-72	-75.636	66
C3	-78	-71	-73.500	66
Average	-80.333	-71.0	-74.722	-

4.4.3. RSSI Dataset

The *RSSI dataset* represents the case where there is not necessarily a line-of-sight between the transmitting luminaire and the receiving smartphone, which is the case in some areas in Business Kitchen since there are pillars, walls and other obstacles attenuating the signal. As was seen in Figure 19, the RSSI seems to behave in a periodic pattern, thus the scans need to be long enough to capture the full periods. Therefore, *PIR EDA dataset* was not used for evaluating the method since the durations of the stays between the walks were generally considered too short, leading to the gathering of *RSSI dataset*, which contained nine scan points, each having a scan duration of one minute. The Samsung Galaxy S8 martphone was used to scan the BLE advertisements, and it was held in hand approximately at the same height, one meter from the ground, during the recording of the dataset. A smartphone stand was not used since it was considered too cumbersome to use also in the actual luminaire identification setting, and the goal of this thesis was to to make configuration easier. During scanning, 58 of the possible 68 luminaires were discovered, the remaining ten did not broadcast any messages at the time.

A coefficient describing the attenuation properties of the environment, usually referred to as n, needed to be defined for the log-distance path loss model. Commonly, n is set from 1.6 to 1.8 indoors with line-of-sight conditions [10] and increased when the signal is attenuated by obstacles. For *RSSI dataset*, n was also estimated with

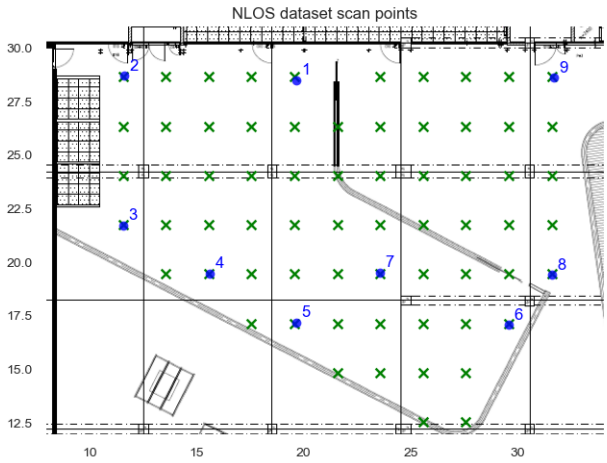

Figure 20. Scan point locations used for RSSI dataset.

the SciPy implementation of the least squares optimization[17] based on the estimated distances to the transmitting luminaires from the scan points and the RSSI values. Since the scan points were estimated from the floorplan by the data gatherer, there is also an estimation error present in comparison to more accurate positioning such as laser measuring tool. The other necessary parameter, RSSI at one meter A, was measured (Table 2), and therefore it was not used as a parameter for fitting the model to the dataset since the calibration measurements were considered more accurate.

The resulting fit with the least squares optimization and the data points for RSSI measurements with distance is presented in Figure 21. According to the optimization result, the value of 1.52 for n seems to minimize the residuals between the model and the measured RSSI. It also seems that a higher RSSI indeed indicates smaller distance, but the variance in the data is high; the average absolute distance, or residual, between the model and measurements is 4.73 m. This result supports the fact that RSSI-based distance estimation is challenging. It is likely that a more complex model could lead to a better fit, but the log-distance path loss model was nevertheless chosen to avoid overfitting since the data represents only the Business Kitchen signal propagation environment and is likely to be different elsewhere.

The reference RSSI at one meter, A, needs to be measured in the space before the luminaire identification process since the luminaire casing, the transmitter location in the luminaire and the used smartphone can affect the RSSI. Another option would be to measure general values for A beforehand. However, the latter option could decrease the performance if the different luminaires or smartphones are not taken into account but would slightly speed up the identification process.

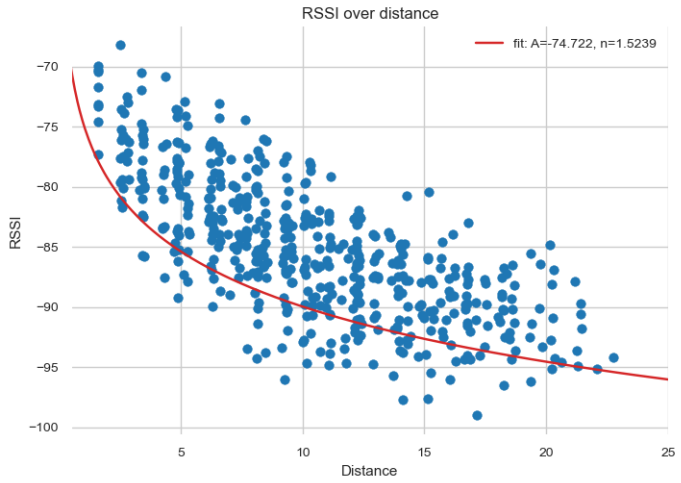

Figure 21. Log-distance path loss model fitted to the *RSSI dataset*.

4.4.4. Evaluation

Figure 22a presents the mean error for n with 0.1 increments and cumulative data for each RSSI scan point, for example, scan point 2 contains the data from scan points 1 and 2, etc. According to the results, the mean error seems to considerably decrease after having more than two points, which supports the trilateration theory. In general, having more scan points seemed to lead to better results except after the 8th scan point when $n < 1{,}6$, which is probably due to the low n value. Also, the mean error tends to increase as n increases when $n < 1{,}6$, which aligns with the knowledge that the optimal n parameter is 1.52 (see Figure 21).

The minimum mean error of 2.79 meters is achieved with $n = 1{,}3$ at seven scan points. However, measuring the performance of the method with the best possible parameter combination is not feasible since n is not known beforehand. As stated previously, values between 1.6 - 1.8 could be selected as n since they are generally used with the log-distance path loss model indoors. When limiting n to $1{,}6 <= n <= 1{,}8$, the minimum mean error is 3.12 meters with $n = 1{,}6$ at nine scan points.

4.5. Discussion

Even though the centroid-based PIR algorithm seemed to provide a better mean error and accuracy, the RSSI-based method could be used as an pre-step to ease the manual luminaire identification. To increase the performance of the PIR-based method, the maximum trigger distance and the smartphone accelerometer data could be utilized. For the RSSI-based method, the orientation of user during the scans could be useful.

[17] https://docs.scipy.org/doc/scipy/reference/generated/scipy.optimize.curve_fit.html

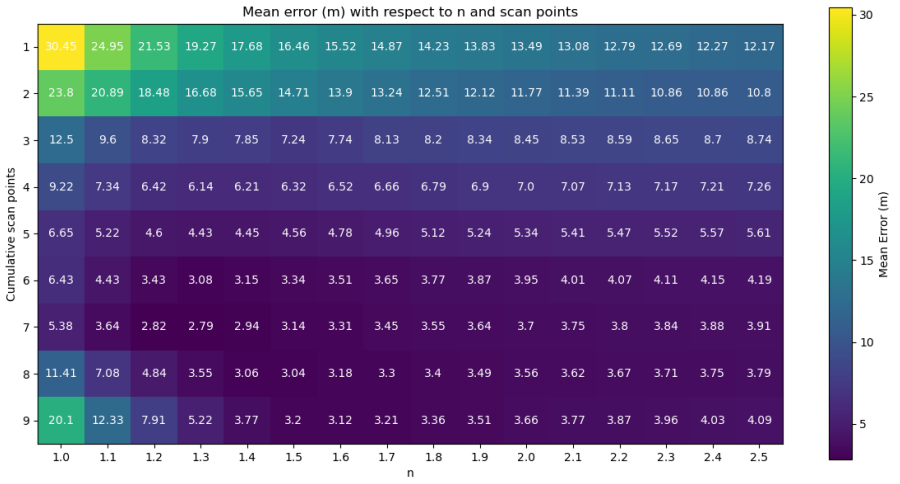

(a) Mean error

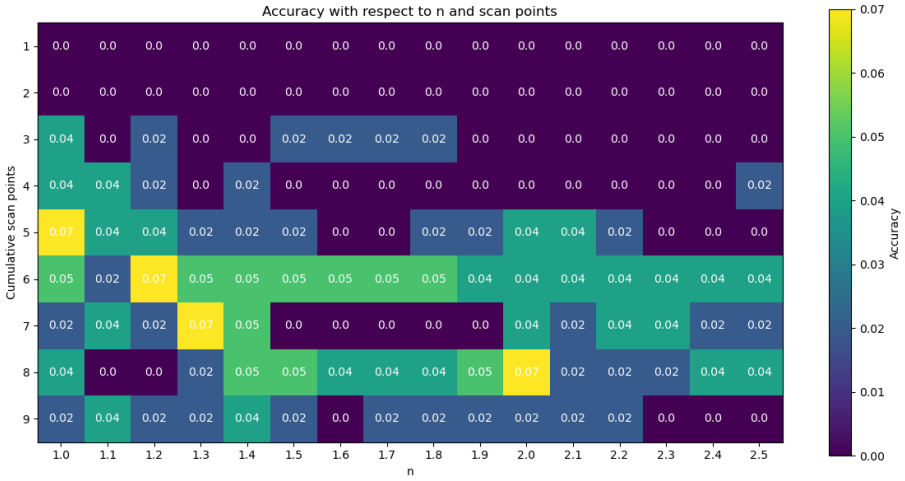

(b) $range_0$

Figure 22. RSSI method performance for *RSSI dataset*.

4.5.1. Comparing PIR Sensor-Based and RSSI-Based Methods

In Business Kitchen, the centroid-based PIR trigger estimation seemed to provide smaller mean error in all conditions *PIR EDA dataset* than RSSI-based method with *RSSI dataset*. Clearly, the challenges presented in Section 2.1.1 with BLE-based RSSI distance estimation have an influence on the results. In optimal conditions, the centroid-based method was able to achieve 100% identification accuracy already after two walks. However, to avoid false PIR sensor triggers, it is required that no one else but the person performing the luminaire identification is present in the space, which is not always possible. This requirement can be loosened slightly by excluding the triggers with a distance greater than the maximum trigger with error between the triggering sensor and the user location at the time. With *PIR EDA dataset* and *PIR optimal dataset* this threshold could be set to 7.5 meters, and if other people stayed at least that far from the person performing the luminaire identification, no false triggers would occur.

The gathered PIR and RSSI data reflect only the conditions in Business Kitchen, and therefore directly inferring the performance of the method in other environments is not possible. However, in general, the performance of the methods should improve the further away the luminaires are from each other. Also, decreasing the PIR sensor trigger radius should lead to better performance in conditions where optimal walking cannot be performed, but it comes with the tradeoff of usability since the sensors are used to turn on the lighting.

Despite the worse accuracy, the RSSI data could augment the PIR-based method by identifying the luminaires that have not yet caused a PIR trigger by utilizing the scans between the walks assuming the scans are long enough. During the identification, these RSSI-based estimates would then eventually be replaced by the PIR-based estimates. The combined RSSI and PIR approach would be helpful especially in the case of large installations where it takes time to cover the whole space with walks. Moreover, the RSSI-based method could be beneficial in a case where the identification accuracy is required to be 100% and performing optimal walks in the space is not possible, thus requiring manual identification to be performed. In this case, a quick RSSI scan with only a couple of scan points could provide a rough estimate of the location of each identifier, which would possibly make the manual identification easier since the identifiers would be nearby and hence easily detected visually.

4.5.2. Future Development

The knowledge of the maximum distance between the PIR sensor and the trigger location, $range_{max}$, could be utilized to avoid identification results that are not possible when mapping the identifiers to the placeholders. For instance, this could be achieved by using a backpropagation algorithm by checking if the placeholder is further away than $range_{max}$ from the estimated location and reverting back to the previous state if this is the case. However, the runtime could considerably increase with the backpropagation approach.

Furthermore, to increase the accuracy of the trigger estimation, a smartphone accelerometer and gyroscope could be used for speed detection during the walks instead of assuming that the speed is constant. For example, Shrestha and Won [31] have achieved a root mean squared error (RMSE) of 0.16m/s for this type of speed detection when the smartphone was held in the participants' pocket. However, holding the smartphone in one's hand, which is required for the data gathering application to be able to end the walk at the correct time, could introduce a swinging motion and therefore could pose a problem.

Also, the developed RSSI-based method could possibly be improved. For instance, the direction the user is facing during scanning could be used to provide some information on the luminaire positions since the user body seems to attenuate the RSSI. Also, different filters, such as Kalman filters, and optimization algorithms could be tried out and inspect their potentiality to increase the performance. Furthermore, the problem could be presented as a simultaneous localisation and mapping (SLAM) problem to remove the effort of inputting the position of the user by using accelerometer and compass information [6]. However, this approach would make the user position an estimate and therefore most likely decrease the performance.

Nevertheless, several factors, such as the walls, furniture and the presence of people, continue to pose a challenge for RSSI-based distance estimation.

5. LIGHTING CONTROL IN COLLABORATIVE SPACES

This chapter presents the process for developing a lighting control prototype to a collaborative space, Business Kitchen, at the University of Oulu. The prototype used uniquely identifiable NFC tags, or switches, to indicate the user position. Tapping the NFC switch with an Android application launched a GUI to enable lighting preference input to a web server that maintained the switch and luminaire state and adjusted the ActiveAhead equipped luminaires accordingly. Possible conflicts were resolved by distance-based averaging between the user preferences. The server was made accessible only through a Wi-Fi access point (AP) to limit the service only to the users in the space. The prototype is presented in Figure 23.

A user evaluation with fourteen participants was conducted and it showed a System Usability Score (SUS) of 76.4 ranking in the top 30 percentile of general SUS scores. The results showed that only five out of fourteen participants noticed that they were controlling shared luminaires. Furthermore, two participants perceived the change of light by the other participant disturbing, eight participants were not bothered with it, and four did not have an opinion on the matter. The study and its results were also published in the journal article [32].

Figure 23. The developed prototype. User 1 ($U1$) has set a preference of 100 and user 2 ($U2$) to 0. The luminaires in between (in green) will be adjusted to 45 since user 2 ($U2$) is a little closer to them. [32], © 2020 by the authors, CC BY 4.0 license (https://creativecommons.org/licenses/by/4.0/).

5.1. Design

User scenarios and requirements for the system are presented in Section 5.1.1 and Section 5.1.2, respectively. Section 5.1.3 continues by describing the reasons behind the made design choices were made and also explores alternative solutions.

5.1.1. User Scenarios

Two scenarios of how the system could work were outlined: one from the perspective of an end user and one from the perspective of a system administrator. Only the functionalities in the end user scenario were fully implemented, but the system administrator scenario was also included to provide a better understanding about the system as a whole.

5.1.1.1. Mark: student

Mark missed today's lecture and wants to watch it online. Business Kitchen is still crowded, but luckily there is a couple of free tables still available. It is 6 p.m. in November, and the luminaires are burning bright. To avoid reflections from the laptop display, he wants to dim the lighting a bit.

Mark sees a lightbulb icon on the table and next to it a QR-code which seems to be a link to a *"Personalized lighting"* - mobile application. He proceeds to download and open up the application. Mark sees a welcome screen which tells him to tap the lightbulb icon on the table with his smartphone, and after tapping the icon, a view with a slider opens in the application. Mark adjusts the lighting level to minimum and the luminaires nearest to him dim accordingly. Now he can start watching the lecture on his laptop.

Another student, Lisa, arrives at the table next to Mark's. Lisa wants to set her lighting preference to maximum since she is reading a book and the current lighting settings feels too dim for her taste. Lisa proceeds to adjust the lighting level the same way as Mark did. Lisa sits in the table right next to Mark, which is why also the two luminaires in between Mark's and Lisa's tables are adjusted halfway from Mark's and Lisa's preferences.

After an hour, Lisa starts to leave and kindly releases the luminaires for others to use by pressing a "Set Default"-button in the mobile application. The two luminaires previously shared by both Mark and Lisa join Mark's preference and dim down. Mark finishes watching the lecture, realizes he is late for dinner and leaves in a hurry. A short while after Mark has left Business Kitchen, the luminaires occupied by Mark return to their default lighting setting. After a couple of minutes, the luminaires turn off according to the ActiveAhead default behaviour since everyone has left the space.

5.1.1.2. John: Business Kitchen administrator

John has been tasked to install a new *"Personalized lighting"* system to Business Kitchen. He has been given a box containing an introductory leaflet to the system, a Raspberry Pi-looking device and a stack of NFC tags with lightbulb icons labelled as *Switches*. The leaflet instructs John to place the Raspberry Pi-looking device to an unreachable location in the space, plug it to a power source and start up a mobile application.

John logs in to the system with admin credentials that came with the leaflet and changes his password. The next view shows the floorplan of Business Kitchen

currently with no *Switches*. John presses the "Add a Switch"-button and sees instructions to tap a *Switch* with his smartphone. A green box on the screen tells him that this *Switch* is not in use yet. John proceeds to select the location for the *Switch* by using the virtual Business Kitchen floorplan and attaches it on the corresponding table in physical Business Kitchen. John continues to install 9 more *Switches* in the same manner. He mostly attaches *Switches* on tables but also to pillars next to sofas.

After a month, John inspects the usage of *Switches*. He notices that two switches, $S1$ and $S2$ have been in low usage. John walks to Business Kitchen to check the situation and notices that the table where $S1$ was placed has been moved. Therefore, John moves $S1$ in the virtual floorplan to match $S1$'s new physical location. However, John cannot find $S2$ from the location it was supposed to be. He only sees the remains of $S2$, meaning someone must have ripped it off. John is not too concerned about the theft since he knows that they can be used to adjust lighting only in the Business Kitchen area. In any case, John chooses to disable $S2$ with the admin view in the application.

5.1.2. Requirements

The following software requirements were summarized based on the user scenario presented in Section 5.1.1.1.

- Tapping a switch with a smartphone at a specific location will allow adjusting lighting intensity at that location.
- Lighting preferences can be inputted using a GUI.
- System can only be used in Business Kitchen area even if the switches are removed and taken elsewhere.
- Pressing a "Set Default"-button adjusts the currently occupied luminaires to the default intensity level in the space. If other people are using the luminaires, the control is transferred to them instead.
- The luminaires should be automatically adjusted to the default intensity level in the space if the user forgets to do it manually a while after the user has left.
- The preference of a person who is closer to the luminaires has more weight in the luminaire output compared to a person who is farther away.

In addition to the software requirements, the physical switches should enable relocation but still be firmly attached to the surface. The material should also be relatively durable to withstand several attachments and non magnetic to avoid interference with the smartphone NFC reader. For the sake of this prototype, a simple NFC sticker based solution was used and developing a long-term solution was left for future work.

Two requirements for Scenario 5.1.1.2 were also summarized and are listed below.

- Administrators can add, relocate and remove switches.
- Administrators can inspect the usage of the switches.

As stated before, these administrator requirements were implemented only to the server but not to the Android client.

5.1.3. Design Choices

Business Kitchen, illustrated in Figure 3, is a public collaborative space containing several tables suitable for group work and facilities for giving speeches and presentations. Anyone visiting the campus during working hours is allowed to work there, although the space seems to be favored by students. This section illustrates the most relevant design choices which were made during the prototype design.

5.1.3.1. Lighting control method

The ActiveAhead equipped luminaires in Business Kitchen are placed evenly to a grid formation to provide general lighting to the space. This means that the luminaires are not targeted to any particular table, hence luminaire sharing with the adjacent tables was thought necessary.

The next step was to decide how much individual luminaire control the users were allowed to have. Krioukov et al. [20] and Zou et al. [19] provided a user interface to adjust all the nearby luminaires individually. However, this approach did not seem to fit well to Business Kitchen due to the high amount of luminaires in the user's proximity, which could potentially lead to confusion in selecting the appropriate luminaires and would also require manual effort in adjusting all the luminaires individually. Therefore, a single input that would adjust all the nearby luminaires at the user location was thought to be a more user-friendly solution, in a similar fashion with Petrushevski [21].

Two device choices for inputting the users' lighting preferences were considered: a smartphone or an embedded board. Due to the public nature of Business Kitchen, a smartphone was selected since the embedded boards might attract some malicious users wanting to steal them. Also, the costs of the embedded boards would scale poorly with the increased amount of users in the space, whereas almost every person visiting the space would most likely have a smartphone.

There was also a possibility to utilize the smartphone illuminance sensors to take the background lighting into account in a similar manner as done by Petrushevski [21]. However, the idea was abandoned since orientating the illuminance sensor would have an effect on the sensor reading and thus the lighting output, meaning that the users would need to have their smartphones constantly facing up on the table, which would prevent all other use of the smartphone.

Distance weighted preference averaging was chosen to resolve the potential conflicts by giving the users closer to the luminaire more weight to its output. After experimenting, it was also noticed that the luminaires roughly more than two meters away from the switch did not have a considerable effect to the lighting and could potentially irritate people who do not use the system. Therefore, the control of the nearby luminaires was restricted to the luminaires within two meters. In the case where there were no other users nearby, the current user was given the full control of the luminaires within the range. To implement the presented conflict resolution model, a component with the knowledge of all luminaire positions and the preferences of the current users were needed. Thus, centralized control was needed.

5.1.3.2. Positioning technology

To enable location based lighting adjustment, the user position needed to be determined. Since the luminaires were installed relatively close to each other with approximately 2 m and 2.3 m distances in between to the x and y directions, the positioning needed to be relatively accurate.

RF (radio frequency) based indoor positioning systems (IPS), i.e., Wi-Fi and BLE when considering smartphones, were determined too inaccurate since they generally achieve 1-2 m accuracy in controlled environments but can perform even worse depending on the factors, such as the amount of collected fingerprints, the up-to-dateness of the the fingerprint database and RF coverage in the area [5]. During the designing of the prototype, a BLE beacon based indoor positioning system was installed to the campus and could have been used for this prototype without having the need to install other systems. However, as in line with the performance of the previous systems [5], it was not considered accurate enough for this use case.

Instead of utilizing an IPS, unique identifiers were chosen to mark the locations where the lighting could be adjusted with a help of the Business Kitchen floorplan. This floorplan based solution was thought to be considerably easier to implement and it would enable getting user feedback regarding the system without a considerable positioning error comparing to IPS-based solutions. On the downside, placing the switches to the space would add some manual effort. Also, the number of locations for lighting adjustment would be limited to the amount of placed switches, whereas IPS-based solutions could potentially provide a continuous lighting adjustment.

The unique identifiers marking the switch locations could be written to NFC tags, as done by Petrushevski [21], but also QR codes could be used for this purpose as done by Krioukov et al. [20]. Ideally, both technologies could be used simultaneously, which would give the user an option to choose based on her preference, but NFC was chosen to be implemented first for the prototype.

5.1.3.3. Authentication and security

Only the people present in Business Kitchen were allowed to adjust the lighting to prevent accidents, misuse and hacking. Therefore, the lighting control server was made accessible only through a local Wi-Fi access point (AP) placed to Business Kitchen, meaning the users were required to join "Business Kitchen" Wi-Fi AP. BLE was also an option for communication between the application and the lighting control server, but Wi-Fi was thought to perform better for a high number of concurrent connections. The drawback of the Wi-Fi based access limitation was that all users' Internet traffic needs to be routed through the AP. If the AP would not provide an Internet access, Android would automatically try to connect to another previously used AP or fall back to cellular connection.

Krioukov et al. [20] and Zou et al. [19] required also credentials for using their systems. The organizational credentials would mitigate the application misuse by being able to identify the user causing trouble and deny the access to the service. Limiting the service only to persons with university credentials did not suit Business

Kitchen well, since it would exclude other visitors than university students or faculty members from using the system, and was therefore not implemented.

Physical hacking in the case for the prototype could mean rewriting, stealing or moving the NFC tags or being able to access or steal the server or the Wi-Fi AP. By default, anyone who had an appropriate smartphone application installed could rewrite the NFC tags, but this was prevented by locking the tags to be read-only before use. Stealing the NFC tags would not be a significant loss due to their cheap price, and since the Wi-Fi connection would be needed, the potential attacker could only control the corresponding switch in the Wi-Fi range. The most obvious and easiest way for the physical hacking would simply be turning off the lights from a physical switch, but this option would be present despite the presence of the prototype. The likelihood for physical hacking was also considered to decrease due to the restrictions to access the space off working hours and the presence of security cameras in the space. If NFC-based physical hacking was to succeed, it would result in the hacker being able to adjust another person's lighting and most likely being an annoyance for the users at worst, and finding the hacker would be relatively easy since the attacker would be in the Wi-Fi range.

To protect the users' privacy, the server component did not store any information where the users could be identified. Only the events for adjusting lighting or setting the lighting to the default level were stored with the information of the used switch and its location, timestamp and the user preference. If the system stored the identifiers representing the users, it would result to a tool for the administrators to inspect when particular identifiers have been in the space. By itself this would not be a problem, but since the service was only accessible from the Wi-Fi range, the administrators would be able to relate the identifiers to real persons by simply walking to the space and watching who is currently using each switch, also revealing all other times when that person has been in the space. Even if the administrators would be trusted with an opportunity to know when each user has been in the space, the Raspberry Pi placed to the space and running the server could be stolen.

Encrypting the messages between the server and the Android client was not considered necessary since the messages did not contain any personal information, and adjusting the lighting in the space was decided to be accessible for everyone in the space anyway. However, transport layer encryption would be recommended for any administrator tasks, for which the regular users do not have access, such as repositioning and adding switches.

5.1.3.4. User presence detection

The arrival of the user was possible to detect with NFC, and for leaving the space, disconnecting the Wi-Fi network was chosen as an indicator. In addition, closing the application was considered leaving the switch. A "Set default"-button meant for the user to indicate that she is leaving and wants to set the lighting back to the default level was also thought necessary if the user wanted to remain in the range of the WiFi but still free the luminaires for others to use. The last user tapping the NFC switch was chosen to given the switch control and override the previous user preference. This functionality was considered useful in the case where a user would forgot to set the

lighting to default level with the "Set default"-button when leaving the space but still staying within the range of Wi-Fi.

The campus BLE-based IPS could also have been utilized for more accurate user presence detection, but it would have also required the user to turn on location and Bluetooth services causing manual effort and increasing battery consumption. As it has been stated previously in Section 3.1.1, the PIR sensors in general are not able to identify the persons, and thus the sensors in the luminaires could not be used for the user presence detection. Timer based solutions were also neglected since they were thought to require too much effort for the user.

5.2. Implementation and Testing

The system consisted of two types of components: a client for the users to adjust the lighting and a server for maintaining the list of current users, updating their preferences and transferring the lighting control commands to the luminaires. The system architecture is presented in Figure 24.

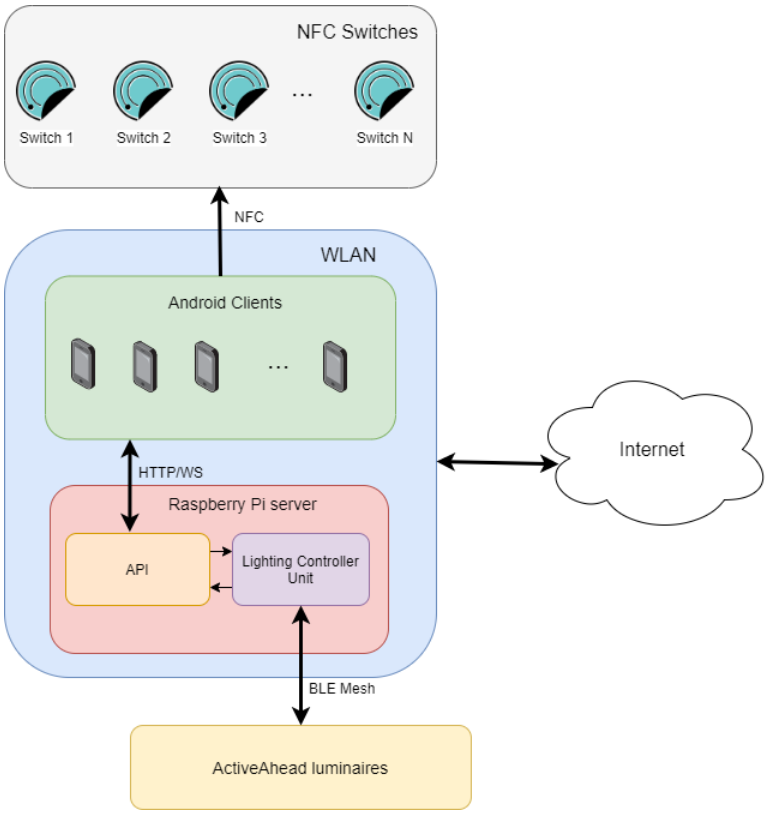

Figure 24. The system architecture.

The client was implemented as an Android mobile application. The reason for this choice was the need to maintain a connection to the server even if the user wanted to turn the smartphone screen off or use other applications. Otherwise, in the case when the connection to the was lost, the lighting intensity would be recalculated even if the user still wanted to maintain her lighting preference. The Android foreground

service[18] solved this problem but required showing a notification to the user that she is still occupying the switch. To the author's best knowledge, maintaining a connection to the server while not interacting with the application was not possible with the web based clients working in a mobile browser application. Furthermore, Material Design components[19] was used for GUI development. The NFC switch is presented in Figure 25a and the GUI for inputting the user lighting preference in Figure 25b.

(a) A switch for prototype.

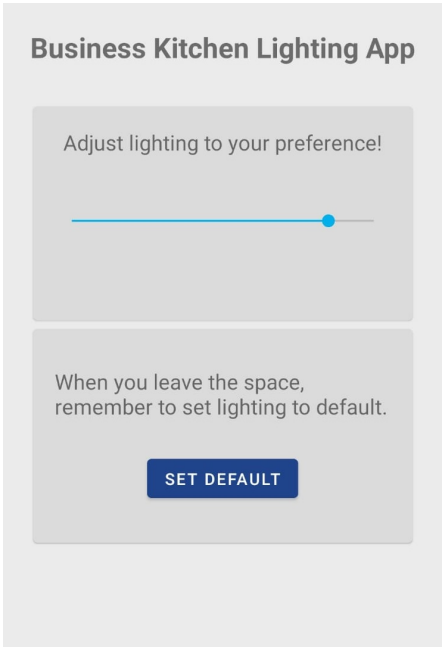

(b) UI adjusting the lighting.

Figure 25. The application enabling personal lighting control. [32], © 2020 by the authors, CC BY 4.0 license (https://creativecommons.org/licenses/by/4.0/).

The server API was implemented with Python and Django web framework[20] and communicated with a SQLite[21] database. Django Channels[22] was utilized to form a Websocket connection between the client and the server indicating an occupation of a switch. Django REST framework[23] was used to implement create, read, update and delete (CRUD) operations for $Switch$ and $Luminaire$ resources authorized only for administrators. The switch actions to modify the lighting level and set the level to the default were authorized for all users in the network. The true positions of the luminaires were derived during luminaire identification presented in Section 3.2 and added to the database with a Python Script.

The lighting controller unit (LCU) ran in another thread and communicated with the luminaire mesh network by an external device provided by Helvar Oy Ab through a Serial interface using Pyserial module[24]. LCU was built to enable a transfer to a

[18] https://developer.android.com/guide/components/services
[19] https://github.com/material-components/material-components-android
[20] https://www.djangoproject.com/
[21] https://www.sqlite.org/index.html
[22] https://channels.readthedocs.io/en/latest/
[23] https://www.django-rest-framework.org/
[24] https://pythonhosted.org/pyserial/

different manufacturer luminaires if needed by overriding set_level and $set\_default$ methods which would adjust the luminaire intensity and return the intensity back to a default level.

The server was deployed to a Raspberry Pi 4, which is a low-cost single-board computer using a Daphne[25] server. Furthermore, an external application was used for reading, writing and locking the NFC switches. The interaction of the components in the system is presented in Figure 26.

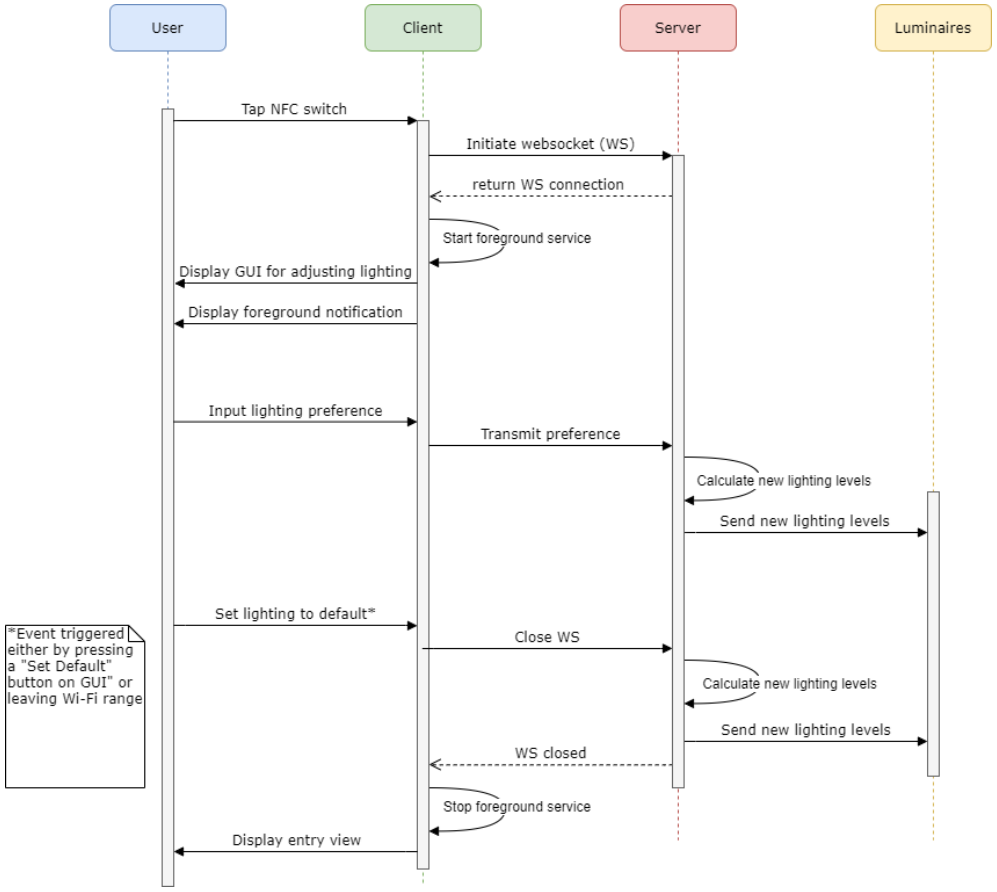

Figure 26. The use case sequence diagram.

The most important server functionality such as the endpoint authorization as well as the distance-based lighting output calculation were unit tested. Also, an integration test simulating the server and LCU behavior with multiple users was implemented. Finally, a manual end-to-end test was performed for the whole system before the user evaluation. Django, Django REST Framework and Django Channels testing tools were used for test automation. The end-to-end tests are further described in Appendix 3.

5.3. Evaluation

The goals of the evaluation were to gather user experiences about the shared lighting control, evaluate system usability and identify potential usability problems. The

[25] https://github.com/django/daphne

evaluation was conducted with seven pairs of participants (thus, overall fourteen participants). Each participant had control of four luminaires: two shared and two of their own. The setup, illustrated in Figure 27, aimed to maximize the effect of the luminaire sharing by placing the switches directly between the luminaires, so that both participants had equal control to the shared luminaires. The participants were first introduced to the system, then the tasks to be performed were given one at a time after accomplishing the previous task. The participants were assigned either a role of Reader or Programmer to make it easier to give instructions. The tasks are listed below:

1. Participants are given smartphones with the Android client installed, NFC disabled and Wi-Fi turned off.
2. Both: open up the application and follow instructions shown in the application. (The application prompts to enable NFC and join Wi-Fi.)
3. *Waiting until both participants have the GUI to adjust lighting open*
4. Reader: adjust preference to minimum (0).
5. Programmer: adjust preference to minimum (0).
6. Reader: adjust preference to maximum (100).
7. Programmer: adjust preference to maximum (100).
8. Reader: adjust preference to half way (50).
9. Programmer: adjust preference to half way (50).
10. Reader: adjust preference to maximum (100)
11. Programmer: adjust preference to minimum (0)
12. Reader: leave Business Kitchen and set lighting back to the default level. Programmer: continue working.
13. *Waiting that the Programmer will see the effect of Reader leaving*
14. *Experiment ends. Both participants fill out the questionnaire.*

After completing the tasks, participants filled out a System Usability Scale (SUS) [33] questionnaire with additional questions related to the shared luminaire control and continuing using the system in the future. Since there were several roof windows in Business Kitchen, the evaluation was conducted at evening time to eliminate the effect of natural lighting. Also, the lighting intensity for the rest of the luminaires, which were not used in the study, was set to the default level (85 on a scale from 0 to 100). The lights in nearby cubicles were turned on. The evaluation setup attempted to maximize the effect of the shared luminaires as can be seen in Figure 27.

5.3.1. System Usability

System usability scale (SUS) [33] was chosen as a usability metric due to its popularity and simplicity. The developed prototype gained a SUS score of 76.4. Generally, the average SUS score is 68 [34]. Thus, the SUS score of the developed prototype ranks in the top 30 percentile [34]. The SUS score distribution with the fourteen participants is presented in more detail in Figure 28.

Half of the participants had not used NFC before, therefore, they needed some practicing to get used to the interface. Two users had particular challenges with using NFC technology and were aided with the tapping of the NFC switch. At the end, only one participant commented that NFC is too difficult to use for this application. [32]

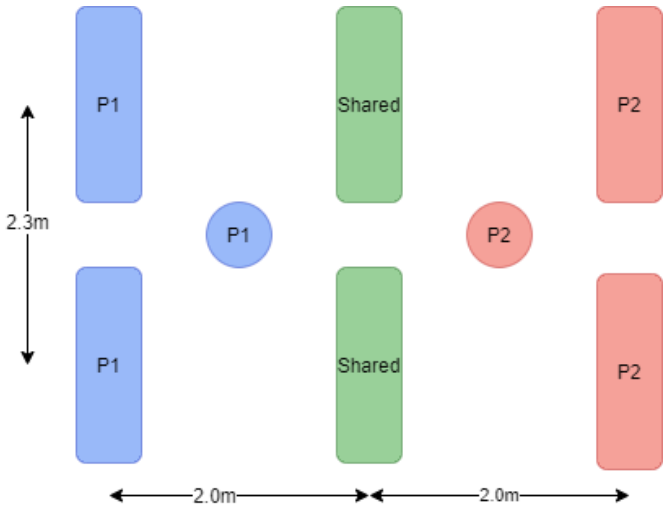

Figure 27. Circles indicate the positions where participants $P1$ and $P2$ sat during the evaluation. $P1$ had the total control of the luminaires marked in blue and $P2$ for the luminaires marked in red. Both participants had equal weight to the shared luminaire control, marked in green.

During the evaluation, it was also observed that users tended to accidentally close the popup instructing to enable NFC and join the Business Kitchen Wi-Fi and therefore be unsure how to proceed. In the case when popup was dismissed, the users were told to open up the application again. After the evaluation, the client was updated to prevent the users accidentally closing the popups.

5.3.2. Experiences on Shared Lighting Control

The results show that five out of fourteen participants did not notice that they were controlling shared luminaires, whereas the rest of the participants did pay attention to the shared control. Moreover, eight participants were not bothered with the change of lighting by the other participants, two participants found the change disturbing, and four did not have an opinion on the matter. Commonly, having different lighting levels in the task, surrounding and background areas does not seem to irritate users [35]. [32]

Seven out of fourteen participants wanted to continue using the system when working in Business Kitchen, whereas three of them considered the default lighting good enough and one of the participants was also afraid to affect the lighting conditions of the other users of the space. The participants also gave comments on desired features, such as changing the lighting temperature. The participants also indicated a desire to use a similar lighting control method in other spaces such as home. [32]

Since the evaluation was limited only to two participants, further research is needed for the group dynamics in luminaire sharing. Also, how the perception of the other participants adjusting lighting changes when the shared luminaires have less effect on the participant's task area, could be studied further.

#	Statement	Strongly disagree	Disagree	Neutral	Agree	Strongly agree	Points
1	I think that I would like to use this system frequently.		4	4	2	4	34
2	I found the system unnecessarily complex.	6	6	1	1		45
3	I thought the system was easy to use.		1	2	4	7	45
4	I think that I would need the support of a technical person to be able to use this system.	8	4			2	44
5	I found the various functions in this system were well integrated.			5	3	6	43
6	I thought there was too much inconsistency in this system.	6	5	3			45
7	I would imagine that most people would learn to use this system very quickly.		1	2	4	7	45
8	I found the system very cumbersome to use.	6	2	3	3		39
9	I felt very confident using the system.		2	1	3	8	45
10	I needed to learn a lot of things before I could get going with this system.	6	6		1	1	43
Total points: 428, Point average = 428/14 ≈ 30.6 Total score: 30.6 * 2.5 = 76.4							

Figure 28. The SUS questionnaire distribution.

5.4. Limitations and Future Work

The required configuration before starting to use the system is one of the most significant limitations. This configuration consists of identifying the luminaires, although it can be made easier by the techniques presented in Section 4, and of positioning the NFC switches both physically and virtually. As stated before, positioning the switches could be avoided by using a BLE or Wi-Fi based indoor positioning system to locate the user, but the locationing accuracy was not considered sufficient. The administrator tasks, namely physical and virtual switch positioning and relocationing, were not in the focus of this thesis and should be defined, implemented and tested further before introducing users as the system administrators.

Moreover, limiting the access to the service through a Wi-Fi access point also meant that all user Internet traffic is routed through the AP requiring the user trusting the organization providing the AP. Wrapping the service to a particular network this way can cause problems in situations where there are multiple different organizations with their own networks but a common workspace for everyone. One potential solution for limiting the service only to a specific area could be to use BLE to broadcast a dynamic one-time password (OTP). The OTP could possibly be broadcasted by the Raspberry Pi with BLE beacon emulation. The clients would then need to continuously scan the

advertised BLE OTP and connect to the server through their mobile network, i.e., the server would need to be made accessible to the Internet. The OTP could change, for example, in every five minutes to mitigate the malicious use and enable detecting the clients who have left the space. The described BLE-based authentication concept needs to be researched further, but it could potentially replace Wi-Fi as making the service available only for the space users. Static BLE OTP broadcasting has already been proposed to include the location to a multi-factor authentication scheme[36]. From the user perspective BLE scanning requires activating location and Bluetooth services [37] but the need to join to the Wi-Fi AP would be removed.

There are also features that could enhance the user experience if implemented. User could have a preset preference value, which would automatically be updated when tapping the NFC switch. This preset could be switch specific or a common preference for all switches. Currently, the user always needs to adjust the lighting to her preference by using the GUI. It would also be possible to make the preset change based on the previous switch usage. The data needed for this kind of system should probably be saved to the client to protect users' privacy, although the non-identifiable lighting preference data stored on the server could be used as a general starting point.

Furthermore, walls, pillars and other lighting obstacles are not currently taken into account by the conflict resolution. Ideally, the users should not be able to adjust the luminaires whose lighting output is covered by these obstacles. This would require inputting the location and the size of the obstacles to the system, possibly by utilizing the floorplan and a GUI to draw the obstacles. On the downside, this would increase the administrator configuration effort.

6. CONCLUSION

This thesis explored two aspects of these smart lighting systems with a help of an ActiveAhead installation at the University of Oulu.

First, the use of the distance information from Bluetooth Low Energy (BLE) broadcasted received signal strength indicators (RSSI) and the passive infrared (PIR) sensor triggers were explored to position the smart luminaires. For the PIR data, a centroid-based location estimation method was developed and evaluated with two datasets, *PIR EDA dataset* and *PIR optimal dataset* reflecting a typical and optimal scenarios of triggering the PIR sensors. The method provided 1.69 and 0.47 meter mean errors at around 10 minutes of configuration for *PIR EDA dataset* and *PIR optimal dataset* respectively.

For the RSSI data, a method consisting of a log-distance path loss distance estimation and mean squared error (MSE) based position optimization was evaluated providing a 3.12 meter mean error assuming a path loss exponent of $n = 1{,}6$ at the maximum of 9 scan points with a duration of one minute. Due to the layout of the space and luminaires and also the unique signal propagation environment, the results cannot be directly generalized to other spaces and should be considered more as a guideline.

Secondly, a lighting control prototype for collaborative environments was designed, implemented and evaluated. The prototype used near-field communication (NFC) tags to indicate the user position and to initiate a lighting preference input using an Android application. The user preferences were transmitted to the local server, which was responsible for the lighting control logic and adjusting the luminaires accordingly. Distance-based averaging between the user preferences was used for resolving potential conflicts. A user evaluation with fourteen participants was conducted indicating a System Usability Score (SUS) of 76.4 ranking in the top 30 percentile of general SUS scores.

7. REFERENCES

[1] Galasiu A.D. & Newsham G.R. (2009) Energy savings due to occupancy sensors and personal controls: A pilot field study. Proceedings of Lux Europa 2009.

[2] Newsham G., Veitch J., Arsenault C. & Duval C. (2004) Effect of dimming control on office worker satisfaction and performance. In: Proceedings of the IESNA annual conference, pp. 19–41.

[3] Pakanen M., Lovén L., Alavesa P., Gilman E., Terken J., Eggen B. & Pirttikangas S. (2018) Design challenges of wellbeing supporting smart environment in collaborative use situations. In: Proceedings of the 2018 ACM International Joint Conference and 2018 International Symposium on Pervasive and Ubiquitous Computing and Wearable Computers, pp. 688–692. DOI: https://doi.org/10.1145/3267305.3267691.

[4] Gadicherla S. (2018-12-10) Data Analysis and Memory Methods for RSS Bluetooth Low Energy Indoor Positioning. G2 pro gradu, diplomityö. URL: http://urn.fi/URN:NBN:fi:aalto-201812146529.

[5] Davidson P. & Piché R. (2016) A survey of selected indoor positioning methods for smartphones. IEEE Communications Surveys & Tutorials 19, pp. 1347–1370. DOI: https://doi.org/10.1109/COMST.2016.2637663.

[6] Bulten W., Van Rossum A.C. & Haselager W.F. (2016) Human slam, indoor localisation of devices and users. In: 2016 IEEE First International Conference on Internet-of-Things Design and Implementation (IoTDI), IEEE, pp. 211–222. DOI: https://doi.org/10.1109/IoTDI.2015.19.

[7] Han G., Jiang J., Zhang C., Duong T.Q., Guizani M. & Karagiannidis G.K. (2016) A survey on mobile anchor node assisted localization in wireless sensor networks. IEEE Communications Surveys & Tutorials 18, pp. 2220–2243. DOI: https://doi.org/10.1109/COMST.2016.2544751.

[8] Android developers, scanresult. URL: https://developer.android.com/reference/android/bluetooth/le/ScanResult#getRssi(). Accessed 19.8.2020.

[9] Li G., Geng E., Ye Z., Xu Y., Lin J. & Pang Y. (2018) Indoor positioning algorithm based on the improved rssi distance model. Sensors 18, p. 2820. DOI: https://doi.org/10.3390/s18092820.

[10] Miranda J., Abrishambaf R., Gomes T., Gonçalves P., Cabral J., Tavares A. & Monteiro J. (2013) Path loss exponent analysis in wireless sensor networks: Experimental evaluation. In: 2013 11th IEEE International Conference on Industrial Informatics (INDIN), IEEE, pp. 54–58. DOI: https://doi.org/10.1109/INDIN.2013.6622857.

[11] Ali A.H., Razak M.R.A., Hidayab M., Azman S.A., Jasmin M.Z.M. & Zainol M.A. (2010) Investigation of indoor wifi radio signal propagation. In: 2010 IEEE

Symposium on Industrial Electronics and Applications (ISIEA), IEEE, pp. 117–119. DOI: https://doi.org/10.1109/ISIEA.2010.5679486.

[12] Kochláň M. & Miček J. (2014) Indoor propagation of 2.4 ghz radio signal propagation models and experimental results. In: The 10th International Conference on Digital Technologies 2014, IEEE, pp. 125–129. DOI: https://doi.org/10.1109/DT.2014.6868703.

[13] Fet N., Handte M. & Marrón P.J. (2013) A model for wlan signal attenuation of the human body. In: Proceedings of the 2013 ACM international joint conference on Pervasive and ubiquitous computing, pp. 499–508. DOI: https://doi.org/10.1145/2493432.2493459.

[14] Wang Y., Yang X., Zhao Y., Liu Y. & Cuthbert L. (2013) Bluetooth positioning using rssi and triangulation methods. In: 2013 IEEE 10th Consumer Communications and Networking Conference (CCNC), IEEE, pp. 837–842. DOI: https://doi.org/10.1109/CCNC.2013.6488558.

[15] Guidara A., Fersi G., Derbel F. & Jemaa M.B. (2018) Impacts of temperature and humidity variations on rssi in indoor wireless sensor networks. Procedia Computer Science 126, pp. 1072–1081. DOI: https://doi.org/10.1016/j.procs.2018.08.044.

[16] Faragher R. & Harle R. (2014) An analysis of the accuracy of bluetooth low energy for indoor positioning applications. In: Proceedings of the 27th International Technical Meeting of The Satellite Division of the Institute of Navigation (ION GNSS+ 2014), vol. 812, vol. 812, pp. 201–210.

[17] Ma Z., Poslad S., Bigham J., Zhang X. & Men L. (2017) A ble rssi ranking based indoor positioning system for generic smartphones. In: 2017 Wireless Telecommunications Symposium (WTS), IEEE, pp. 1–8. DOI: https://doi.org/10.1109/WTS.2017.7943542.

[18] Snyman J.A. (2005) Practical mathematical optimization. Springer.

[19] Zou H., Zhou Y., Jiang H., Chien S.C., Xie L. & Spanos C.J. (2018) Winlight: A wifi-based occupancy-driven lighting control system for smart building. Energy and Buildings 158, pp. 924 – 938. DOI: https://doi.org/10.1016/j.enbuild.2017.09.001.

[20] Krioukov A., Dawson-Haggerty S., Lee L., Rehmane O. & Culler D. (2011) A living laboratory study in personalized automated lighting controls. In: Proceedings of the Third ACM Workshop on Embedded Sensing Systems for Energy-Efficiency in Buildings, BuildSys '11, Association for Computing Machinery, p. 1–6. DOI: https://doi.org/10.1145/2434020.2434022.

[21] Petrushevski F. (2012) Personalized lighting control based on a space model. In: Proceedings of the 2012 ACM Conference on Ubiquitous Computing, UbiComp '12, Association for Computing Machinery, p. 568–571. DOI: https://doi.org/10.1145/2370216.2370311.

[22] Chandrakar N., Kaul S., Mohan M., Vamsi C.S. & Prabhu K. (2015) Nfc based profiling of smart home lighting system. In: 2015 International Conference on Industrial Instrumentation and Control (ICIC), IEEE, pp. 338–341. DOI: https://doi.org/10.1109/IIC.2015.7150764.

[23] Fraden J. (2004) Handbook of modern sensors: physics, designs, and applications. Springer Science & Business Media, 267-270 p.

[24] Pir motion sensor. URL: https://cdn-learn.adafruit.com/downloads/pdf/pir-passive-infrared-proximity-motion-sensor.pdf. Accessed 19.8.2020.

[25] Teixeira T., Dublon G. & Savvides A. (2010) A survey of human-sensing: Methods for detecting presence, count, location, track, and identity. ACM Computing Surveys 5, pp. 59–69.

[26] Activeahead sense (5630) datasheet. URL: https://helvar.com/wp-content/uploads/2020/06/5630_DATASHEET_EN.pdf. Accessed 12.08.2020.

[27] Bluetooth S. (2010), Specification of the bluetooth system-covered core package version: 4.0.

[28] Baert M., Rossey J., Shahid A. & Hoebeke J. (2018) The bluetooth mesh standard: An overview and experimental evaluation. Sensors 18, p. 2409. DOI: https://doi.org/10.3390/s18082409.

[29] Gomez C., Oller J. & Paradells J. (2012) Overview and evaluation of bluetooth low energy: An emerging low-power wireless technology. Sensors 12, pp. 11734–11753. DOI: https://doi.org/10.3390/s120911734.

[30] Darroudi S.M. & Gomez C. (2017) Bluetooth low energy mesh networks: A survey. Sensors 17, p. 1467. DOI: https://doi.org/10.3390/s17071467.

[31] Shrestha A. & Won M. (2018) Deepwalking: Enabling smartphone-based walking speed estimation using deep learning. In: 2018 IEEE Global Communications Conference (GLOBECOM), IEEE, pp. 1–6. DOI: https://doi.org/10.1109/GLOCOM.2018.8647857.

[32] Gilman E., Tamminen S., Yasmin R., Ristimella E., Peltonen E., Harju M., Lovén L., Riekki J. & Pirttikangas S. (2020) Internet of things for smart spaces: A university campus case study. Sensors 20, p. 3716. DOI: https://doi.org/10.3390/s20133716.

[33] Brooke J. et al. (1996) Sus-a quick and dirty usability scale. Usability evaluation in industry 189, pp. 4–7. DOI: https://doi.org/10.1201/9781498710411-35.

[34] Sauro J. (2018), 5 ways to interpret a sus score. URL: https://measuringu.com/interpret-sus-score/. Accessed 08.08.2020.

[35] de Bakker C., Aarts M., Kort H. & Rosemann A. (2018) The feasibility of highly granular lighting control in open-plan offices: Exploring the comfort and energy saving potential. Building and Environment 142, pp. 427–438. DOI: https://doi.org/10.1016/j.buildenv.2018.06.043.

[36] van Rijswijk-Deij R. (2010) Simple location-based one-time passwords. Utrecht: Technical Paper .

[37] Bluetooth low energy overview. URL: https://developer.android.com/guide/topics/connectivity/bluetooth-le#terms. Accessed 19.8.2020.

8. APPENDICES

Appendix 1 PIR centroid algorithm results for *PIR EDA dataset*
Appendix 2 PIR centroid algorithm results for *PIR optimal dataset*
Appendix 3 End-to-end test cases for the lighting control prototype

Walk	$range_0$	$range_1$	$range_2$	$range_3$	Mean error (m)	Duration (min:s)
0	0.000	0.000	0.000	0.000	1.820	00:08
5	0.032	0.270	0.476	0.619	2.209	02:17
10	0.286	0.825	0.889	0.905	1.899	04:12
15	0.333	0.746	0.873	0.921	1.803	06:11
20	0.349	0.778	0.857	0.905	1.730	08:13
25	0.317	0.762	0.857	0.873	1.717	10:53
30	0.444	0.937	0.952	0.952	1.579	12:41
35	0.492	0.905	0.937	0.952	1.628	15:41
40	0.381	0.841	0.937	0.952	1.560	18:39
45	0.333	0.810	0.921	0.952	1.566	20:41
50	0.381	0.889	0.937	0.968	1.545	24:52
55	0.444	0.873	0.937	0.968	1.511	26:33
60	0.460	0.873	0.905	0.952	1.488	29:21
65	0.508	0.952	0.952	0.984	1.527	31:17
70	0.508	0.952	0.952	0.984	1.519	33:08
75	0.492	0.921	0.921	0.984	1.515	35:07
80	0.587	0.905	0.937	0.968	1.525	36:42
85	0.540	0.889	0.937	0.968	1.520	38:42
90	0.429	0.905	0.921	0.968	1.526	41:01
95	0.444	0.905	0.921	0.968	1.503	42:27
100	0.508	0.937	0.952	0.984	1.497	44:49
105	0.508	0.937	0.968	0.984	1.501	47:14
110	0.524	0.921	0.952	0.984	1.489	49:27
115	0.603	0.937	0.952	0.984	1.475	51:24
120	0.619	0.937	0.968	0.984	1.460	53:32
125	0.603	0.921	0.937	0.984	1.458	55:27
130	0.603	0.921	0.937	0.984	1.434	57:29
135	0.524	0.889	0.905	1.000	1.417	59:23
140	0.492	0.905	0.921	0.968	1.428	61:33
145	0.492	0.921	0.921	0.984	1.426	62:42
150	0.556	0.952	0.952	1.000	1.413	64:54
155	0.508	0.889	0.905	1.000	1.408	66:53
160	0.492	0.921	0.968	1.000	1.404	68:59
165	0.460	0.937	0.968	1.000	1.408	70:28
170	0.571	0.921	0.968	1.000	1.408	72:46
175	0.571	0.937	0.968	1.000	1.390	76:02
180	0.556	0.921	0.968	1.000	1.392	78:13
185	0.524	0.905	0.952	0.968	1.391	79:50

Walk	$range_0$	$range_1$	$range_2$	$range_3$	Mean error (m)	Duration (min:s)
0	0.333	0.333	1.0	1.0	5.635	00:26
1	1.000	1.000	1.0	1.0	0.192	00:57
2	0.667	1.000	1.0	1.0	1.707	01:26
3	1.000	1.000	1.0	1.0	0.477	01:58
4	0.667	1.000	1.0	1.0	1.096	02:29
5	1.000	1.000	1.0	1.0	0.350	03:01
6	1.000	1.000	1.0	1.0	0.682	03:31
7	1.000	1.000	1.0	1.0	0.307	04:07
8	1.000	1.000	1.0	1.0	0.701	04:39
9	1.000	1.000	1.0	1.0	0.348	05:15
10	1.000	1.000	1.0	1.0	0.727	05:46
11	1.000	1.000	1.0	1.0	0.307	06:23
12	1.000	1.000	1.0	1.0	0.642	06:55
13	1.000	1.000	1.0	1.0	0.363	07:35
14	1.000	1.000	1.0	1.0	0.570	08:11
15	1.000	1.000	1.0	1.0	0.500	08:45
16	1.000	1.000	1.0	1.0	0.656	09:17
17	1.000	1.000	1.0	1.0	0.484	09:51
18	1.000	1.000	1.0	1.0	0.559	10:23
19	1.000	1.000	1.0	1.0	0.418	10:59
20	1.000	1.000	1.0	1.0	0.535	11:31
21	1.000	1.000	1.0	1.0	0.486	12:04
22	1.000	1.000	1.0	1.0	0.564	12:33
23	1.000	1.000	1.0	1.0	0.471	13:05
24	1.000	1.000	1.0	1.0	0.600	13:38
25	1.000	1.000	1.0	1.0	0.499	14:16
26	1.000	1.000	1.0	1.0	0.603	14:47
27	1.000	1.000	1.0	1.0	0.528	15:24
28	1.000	1.000	1.0	1.0	0.657	15:54
29	1.000	1.000	1.0	1.0	0.501	16:27
30	1.000	1.000	1.0	1.0	0.617	17:01
31	1.000	1.000	1.0	1.0	0.475	17:36
32	1.000	1.000	1.0	1.0	0.582	18:05
33	1.000	1.000	1.0	1.0	0.482	18:42
34	1.000	1.000	1.0	1.0	0.586	19:12
35	1.000	1.000	1.0	1.0	0.466	19:43

Type	Description	Result
Manual end-to-end test including the whole system	User opens up the mobile application. The application prompts the user to enable NFC. The user enables NFC. The application instructs the user to tap the NFC switch. The user taps the switch. The application prompts the user to join Business Kitchen Wi-Fi. The user joins the Business Kitchen Wi-Fi. The application shows the user a GUI to adjust the lighting at the location of the switch. The user adjusts the lighting to her preference and the nearby luminaires react accordingly. The user presses the "Set Default"-button. The luminaires return back to the default level.	PASS
The server end-to-end test with multiple users	Luminaire $L1$ is positioned at (1,3), luminaire $L2$ at(3,2) and luminaire $L3$ at (2,2). Switch $S1$ is positioned at (2,3) and Switch $S2$ at (3,3). Switches have an effect on the luminaires within 2 meters, and so $S1$ affects luminaires $L1$, $L2$ and $L3$ and $S2$ luminaires $L1$ and $L2$. User $U1$ sets $S1$ to 50, Lighting Control Unit (LCU) sets $L1$, $L2$, $L3$ to 50 also. User $U2$ sets $S2$ to 5, LCU sets $L2$ and $L3$ to 25 and 30 respectively. $U1$ sets $S1$ to 5, LCU sets $L1$, $L2$ and $L3$ to 5 also. $U1$ leaves and lighting is recalculated: LCU sets $L1$ to the default level of 85 and $L2$ and $L3$ to 5. $U2$ leaves, LCU sets $L2$ and $L3$ to the default level.	PASS